

PNAS

www.pnas.org

Supplementary Information for

Massive formation of early diagenetic dolomite in the Ediacaran ocean: Constraints on the “dolomite problem”

Biao Chang, Chao Li, Deng Liu, Ian Foster, Aradhna Tripati, Max K. Lloyd, Ingrid Maradiaga, Genming Luo, Zhihui An, Zhenbing She, Shucheng Xie, Jinnan Tong, Junhua Huang, Thomas J. Algeo, Timothy W. Lyons, Adrian Immenhauser

Chao Li

Email: chaoli@cug.edu.cn

Junhua Huang

Email: jhuang@cug.edu.cn

This PDF file includes:

Figures S1 to S12

Tables S1 to S5

SI References

Supplementary figures

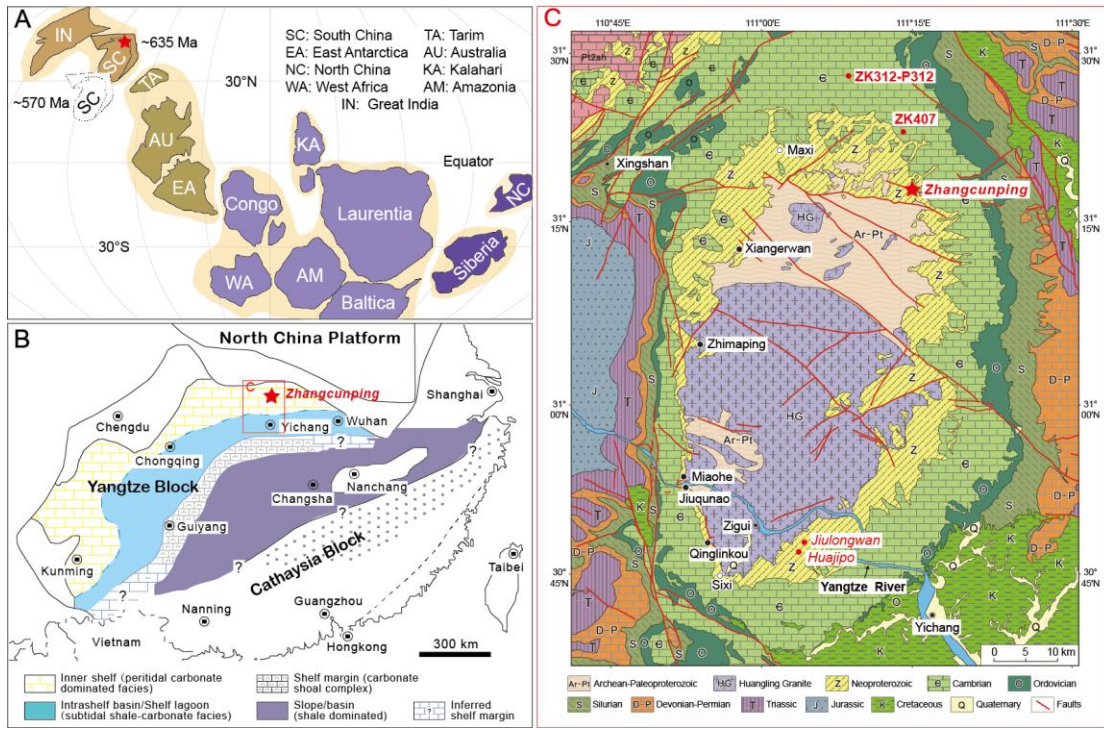


Fig. S1. Geological setting of the Ediacaran Doushantuo Formation in South China. (A) Location of South China (SC) in a global reconstruction at ca. 635 Ma and its latitudinal change from ca. 635 to ca. 570 Ma (dashed outline) (1). (B) Main facies of the Doushantuo Formation on the Yangtze Block. Location of Zhangcunping town shown as red star. (C) Geological map of the Yangtze Gorges area showing locations of drillcores ZK312-P312 and ZK407 as red dots close to Zhangcunping town. The Jiulongwan and Huajipo outcrop sections, which were previously studied for dolomite $T_{\Delta 47}$ (2, 3), are also marked with red dots. Subfigures (A-C) are modified from refs. 4, 5, and 6. Copyright (2013, 2011, and 2015), respectively, with permission from Elsevier.

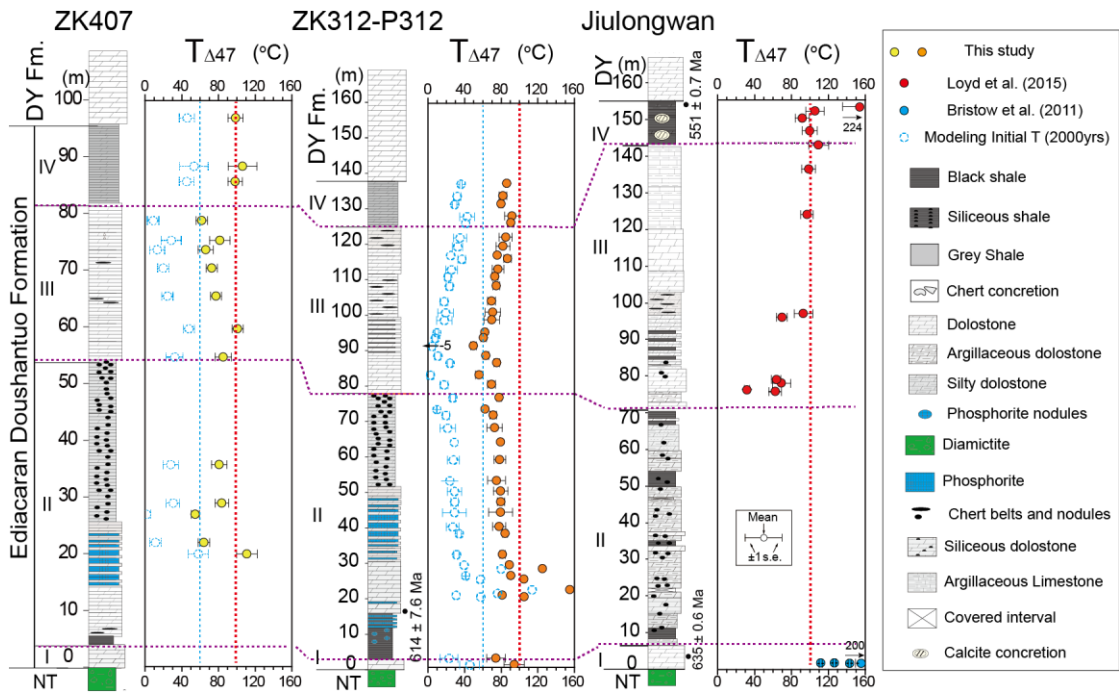


Fig. S2. Dolomite clumped isotope temperature ($T_{\Delta 47}$) profiles of the Ediacaran Doushantuo Formation in the ZK312-P312 and ZK407 drillcores, compared to a previously reported profile for the Jiulongwan section (2, 3). The initial $T_{\Delta 47}$ data (i.e., blue circles) are based on a solid-state reordering model assuming a peak heating temperature (T) of 270 °C for 2000 years. See main text for details regarding stratigraphic correlations and the solid-state reordering model. I-IV = Members I to IV of the Doushantuo Formation, NT = Nantuo, DY = Dengying, Fm. = Formation.

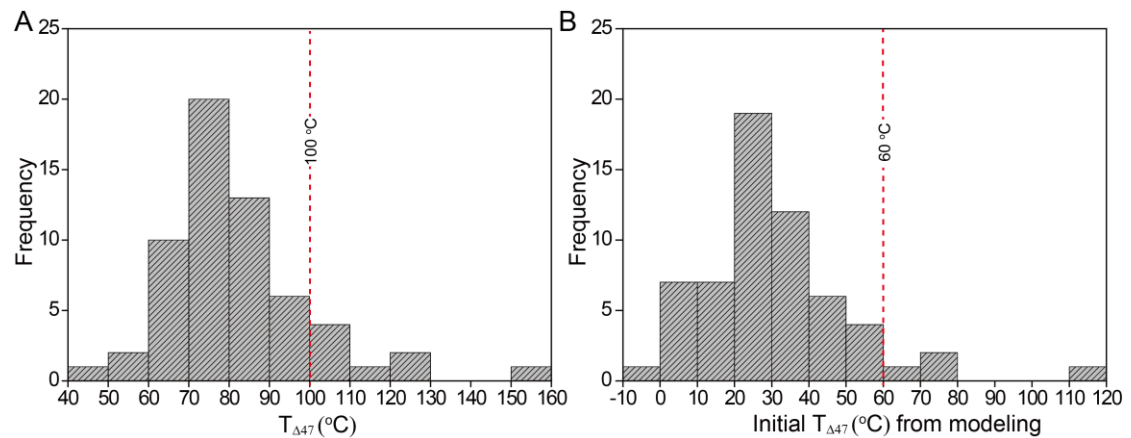
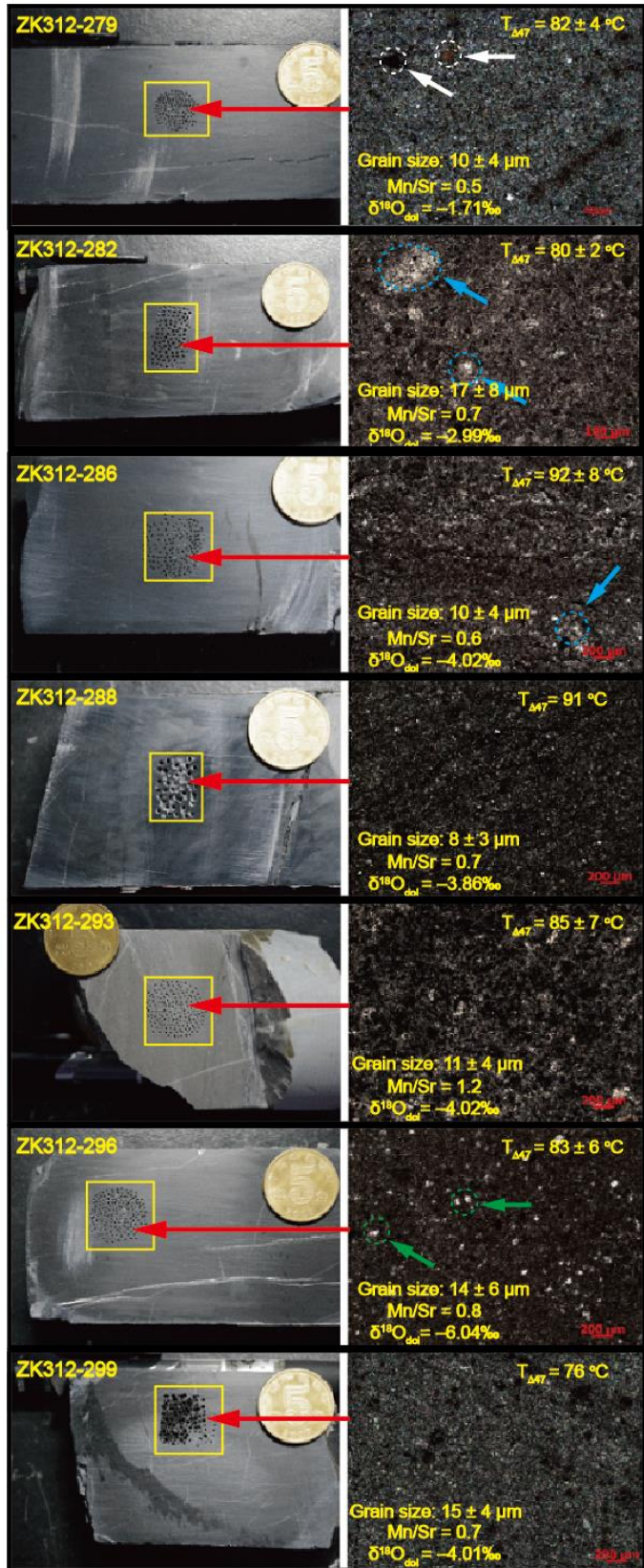


Fig. S3. Histograms of measured $T_{\Delta 47}$ values of Doushantuo dolomite (A) and of their initial $T_{\Delta 47}$ values from modeling (B). The initial $T_{\Delta 47}$ values from modeling are based on a solid-state reordering model assuming a hydrothermal event with a peak heating of 270°C for 2000 years. See text for modeling details.

A Core sample and corresponding photomicrograph



Lithologic description

ZK312-279:
 Microcrystalline dolomite
 and dolosparite containing
 phosphatic grains
 (white arrows)

ZK312-282:
 Microcrystalline dolomite
 containing dolosparite
 particles (blue arrows) and
 dispersed phosphatic grains

ZK312-286:
 Microcrystalline dolomite
 containing dolosparite
 particles (blue arrows) and
 dispersed phosphatic grains

ZK312-288:
 Microcrystalline dolomite
 and dolosparite containing
 phosphatic grains

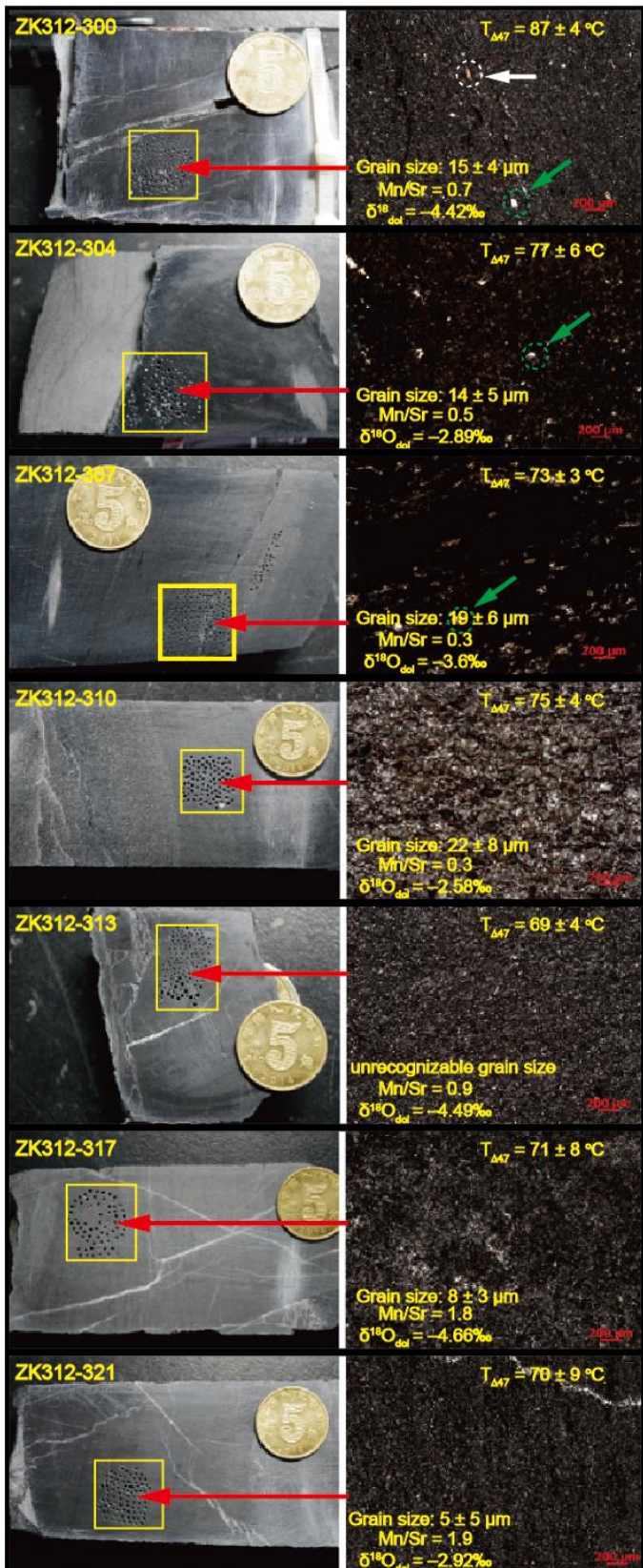
ZK312-293:
 Microcrystalline dolomite
 containing dolosparite
 patches and dispersed
 phosphatic patches

ZK312-296:
 Microcrystalline dolomite
 containing dolosparite and
 calcisparite patches
 (green arrows) and dispersed
 phosphatic grains

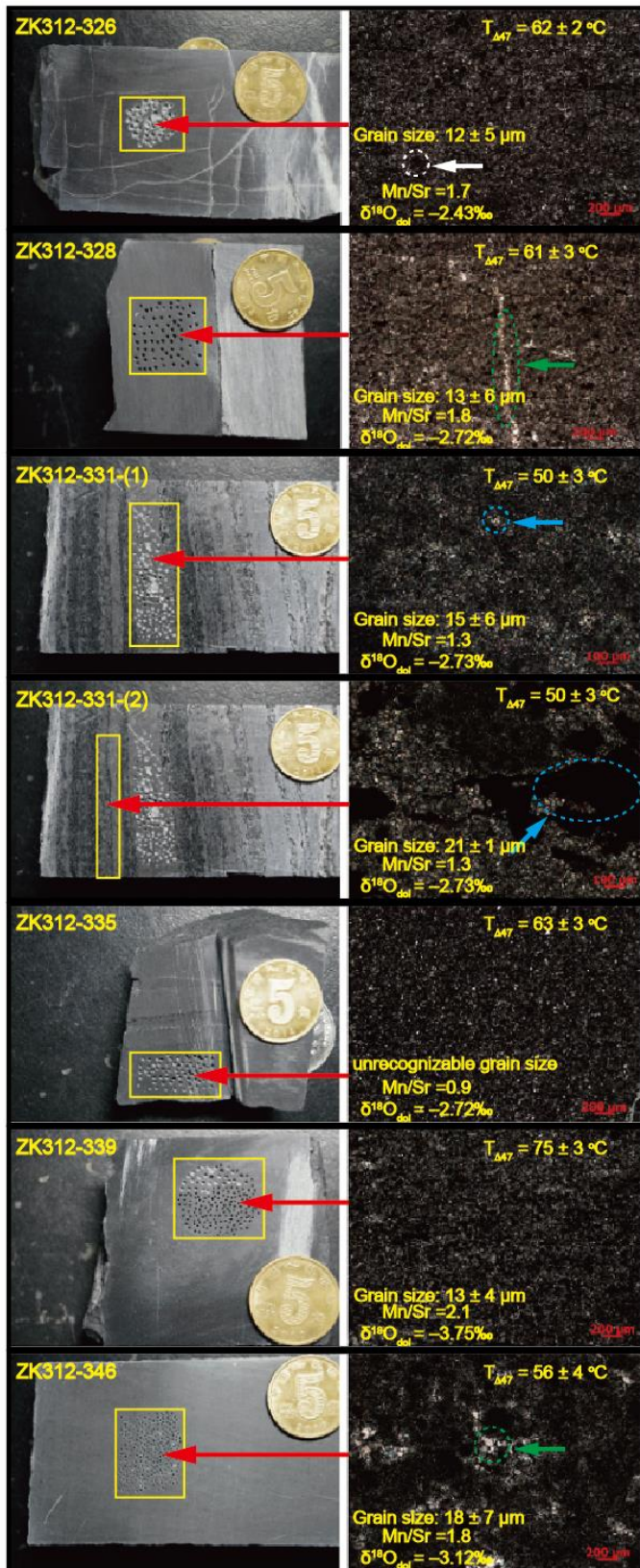
ZK312-299:
 Microcrystalline dolomite
 containing dolosparite particles
 and phosphatic grains

B Core sample and corresponding photomicrograph

Lithologic description



C Core sample and corresponding photomicrograph



Lithologic description

ZK312-326:
 Microcrystalline dolomite and dolosparite containing phosphatic grains (white arrows)

ZK312-328:
 Microcrystalline dolomite and dolosparite containing sparry calcite patches (green arrows) and dispersed phosphatic grains

ZK312-331-(1):
 Microcrystalline dolomite containing dolosparite particles (blue arrows) and dispersed phosphatic grains

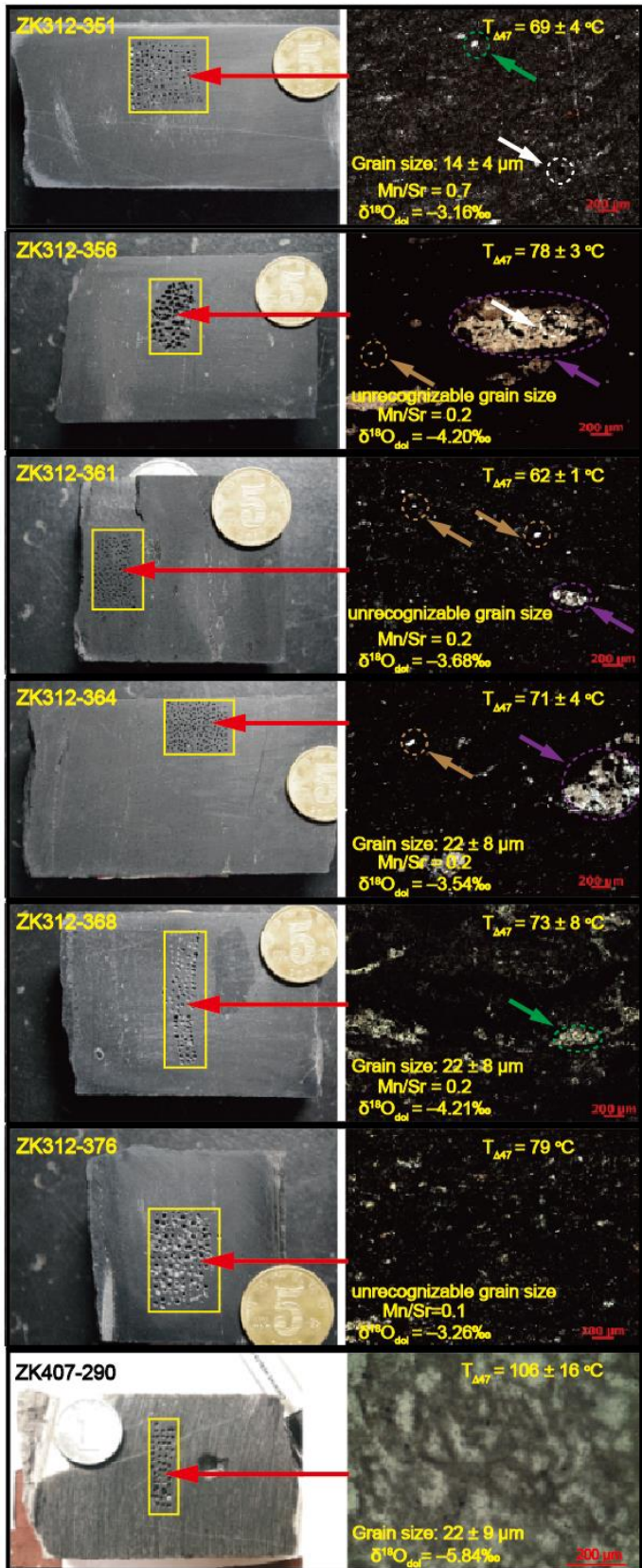
ZK312-331-(2):
 Microcrystalline dolomite and dolosparite containing dolosparite particles and phosphatic grains (blue arrows)

ZK312-335:
 Microcrystalline dolomite and dolosparite containing dispersed phosphatic grains

ZK312-339:
 Microcrystalline dolomite and dolosparite containing dispersed phosphatic grains

ZK312-346:
 Microcrystalline dolomite and dolosparite containing sparry calcite patches (green arrows) and phosphatic grains

D Core sample and corresponding photomicrograph



Lithologic description

ZK312-351:
Microcrystalline dolomite and dolosparite containing calc sparite (green arrows) phosphatic particles (white arrows)

ZK312-356:
Microcrystalline dolomite containing chalcedony block (purple arrows) and dispersed phosphatic particles (white arrows) and pyrite (brown arrows)

ZK312-361:
Microcrystalline dolomite containing chalcedony block (purple arrows) and pyrite (brown arrows)

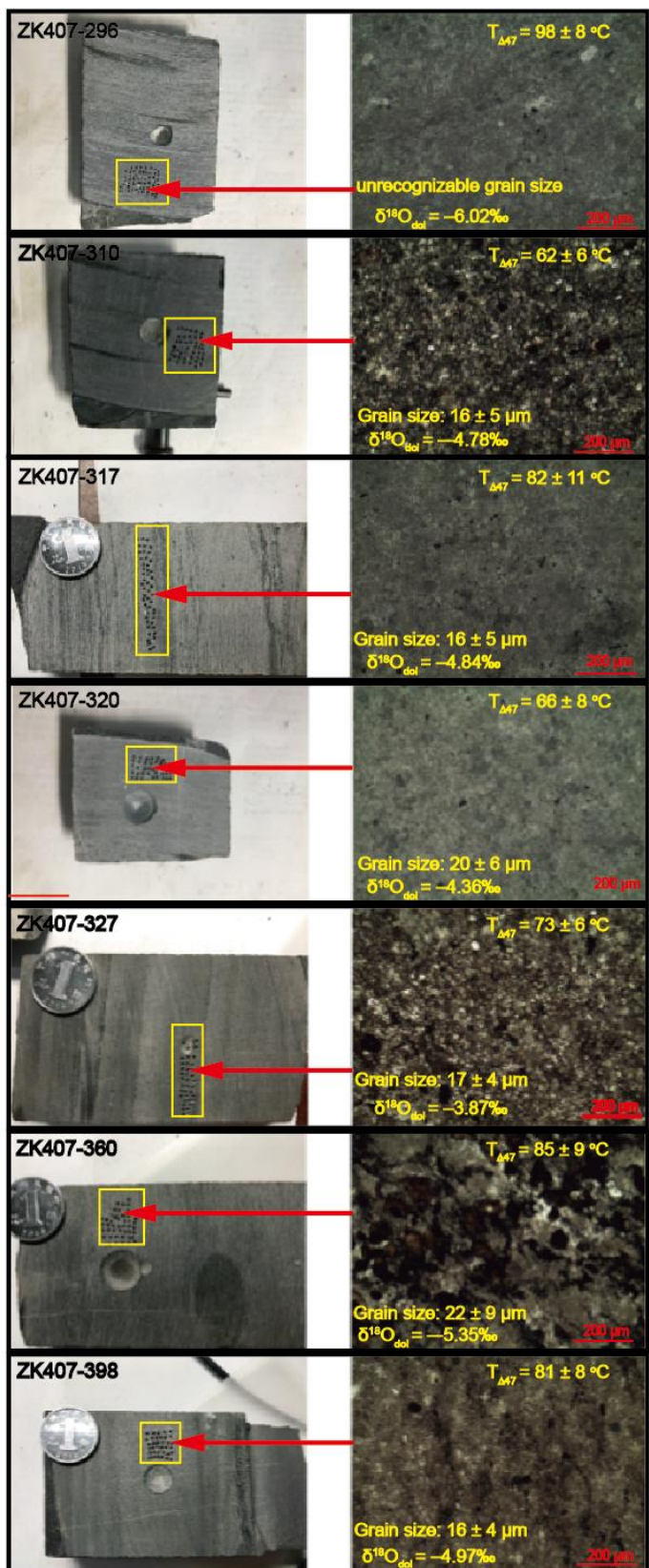
ZK312-364:
Microcrystalline dolomite containing chalcedony block (purple arrows) and pyrite (brown arrows)

ZK312-368:
Microcrystalline dolomite containing calc sparite (green arrows) and dispersed phosphatic grains

ZK312-376:
Microcrystalline dolomite containing calc sparite and dispersed phosphatic grains

ZK407-290:
Microcrystalline dolomite and dolosparite containing dispersed phosphatic particles

E Core sample and corresponding photomicrograph



Lithologic description

ZK407-296:
Microcrystalline dolomite
containing phosphatic particles

ZK407-310:
Microcrystalline dolomite
and dolosparite containing
phosphatic particles

ZK407-317:
Microcrystalline dolomite
containing phosphatic particles

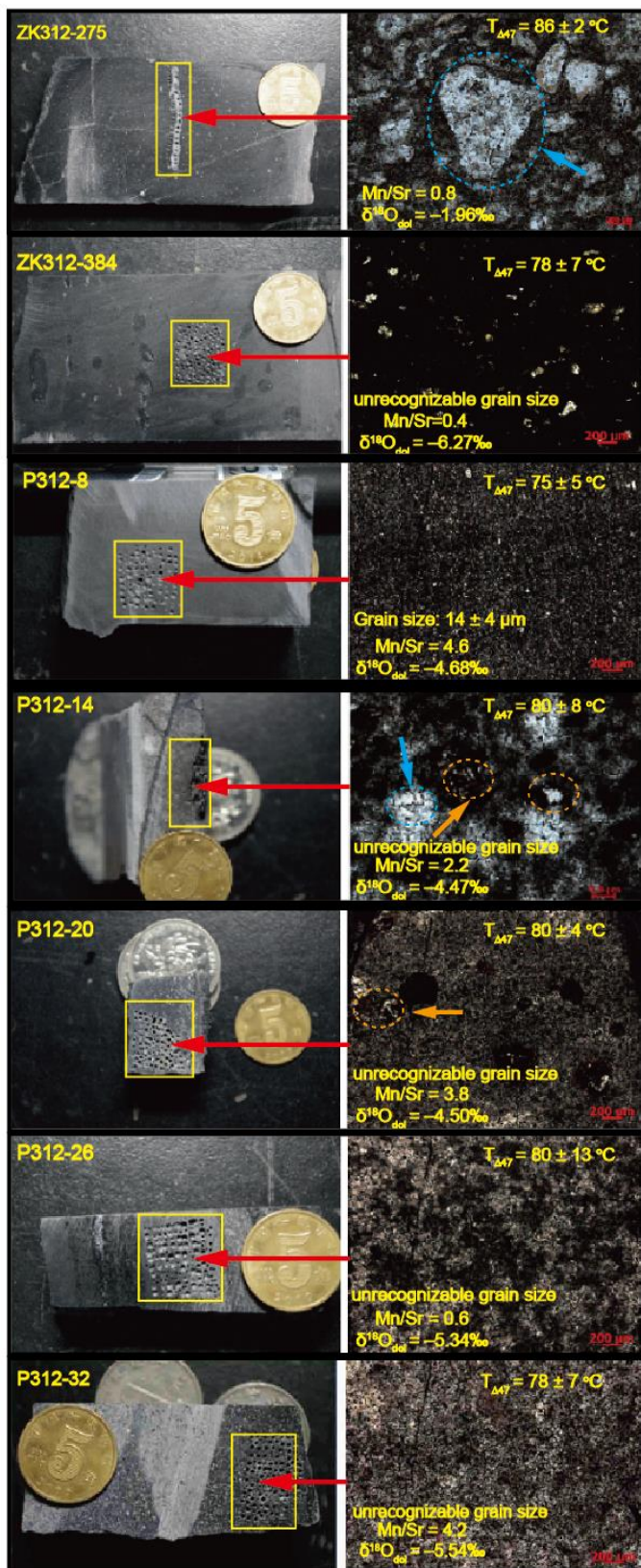
ZK407-320:
Microcrystalline dolomite
containing
dispersed phosphatic grains

ZK407-327:
Microcrystalline dolomite and
dolosparite containing
phosphatic particles

ZK407-360:
Microcrystalline dolomite
and dolosparite, containing
dispersed phosphatic particles

ZK407-398:
Microcrystalline dolomite
containing dispersed
phosphatic particles

F Core sample and corresponding photomicrograph



Lithologic description

ZK312-275:

Microcrystalline dolomite and dolosparite, containing large chalcedony block, Ca and Si intergrowth (blue arrows)

ZK312-384:

Microcrystalline dolomite containing dolosparite particles and phosphatic grains

P312-8:

Microcrystalline dolomite and dolosparite containing phosphatic particles

P312-14:

Microcrystalline dolomite containing dolosparite particles (blue arrows) and dispersed phosphatic patches. Phosphatic debris carbonatization (orange arrows)

P312-20:

Microcrystalline dolomite and dolosparite containing dispersed phosphatic patches. Phosphatic debris carbonatization (orange arrows)

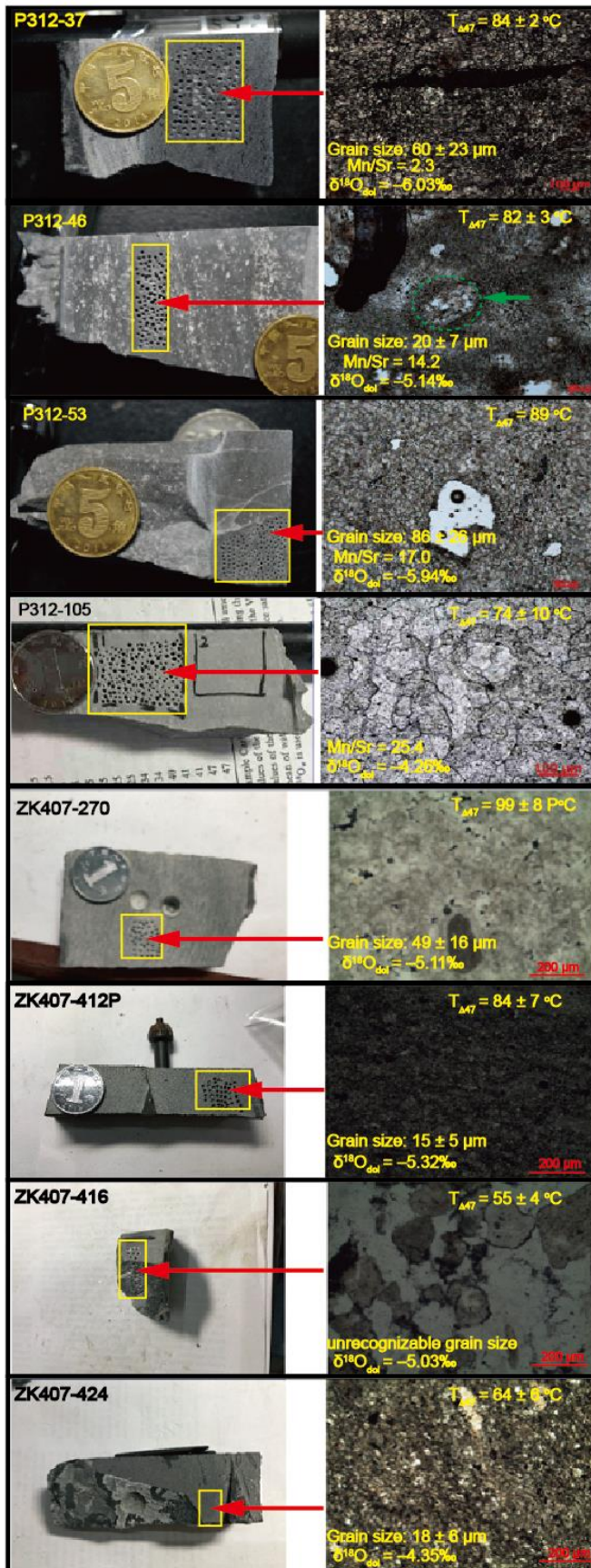
P312-26:

Microcrystalline dolomite and dolosparite containing large dispersed phosphatic particles

P312-32:

Microcrystalline dolomite and dolosparite particles containing dispersed phosphatic particles

G Core sample and corresponding photomicrograph



Lithologic description

P312-37:
Microcrystalline dolomite and dolosparite particles containing dispersed phosphatic particles

P312-46:
Microcrystalline dolomite and dolosparite, containing large calcited phosphatic patches (blue arrows)

P312-53:
Microcrystalline dolomite and dolosparite, containing phosphatic patches

P312-105:
Microcrystalline dolomite and dolosparite

ZK407-270:
Microcrystalline dolomite and dolosparite containing phosphatic particles

ZK407-412:
Microcrystalline dolomite and dolosparite containing phosphatic particles

ZK407-416:
Microcrystalline dolomite and dolosparite containing phosphatic particles

ZK407-424:
Microcrystalline dolomite and dolosparite containing phosphatic particles

Fig. S4. Drillcore segments and corresponding photomicrographs of sampled areas in ZK312-P312 and ZK407 drillcores, including well-preserved samples (*A-E*) and potentially diagenetically altered samples (*F-G*). Geochemical proxies for diagenesis (i.e., Mn/Sr, $\delta^{18}\text{O}_{\text{dol}}$, and grain size) and corresponding $T_{\Delta 47}$ data are shown, as available. Scale: the 1-yuan, 5-jiao and 1-jiao coins have diameters of 2.5 cm, 2.0 cm and 1.8 cm, respectively.

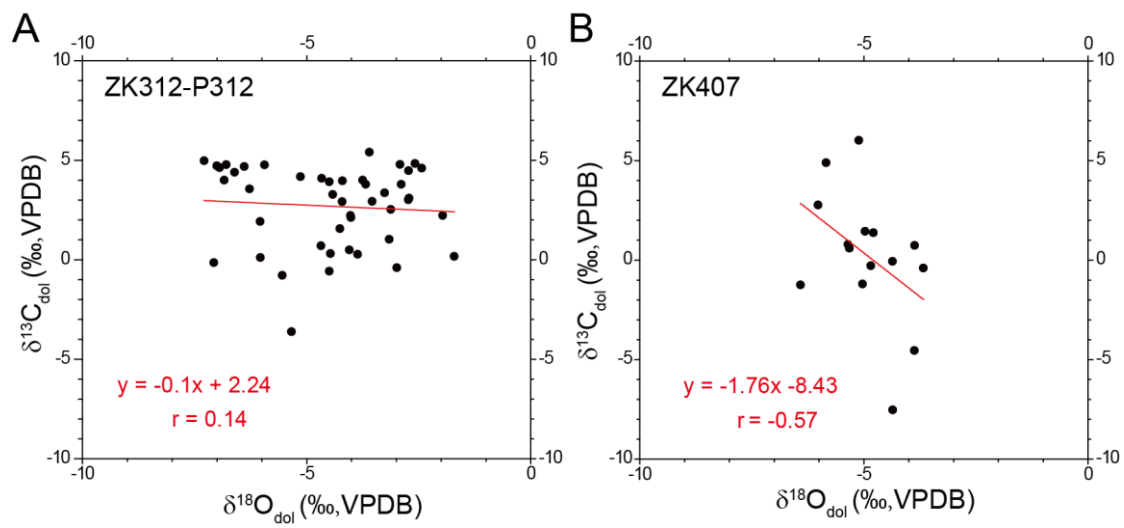


Fig. S5. Crossplots of paired carbon ($\delta^{13}\text{C}_{\text{dol}}$) and oxygen isotope ($\delta^{18}\text{O}_{\text{dol}}$) compositions of Doushantuo dolomite samples from the ZK312-P312 (A) and ZK407 drillcores (B).

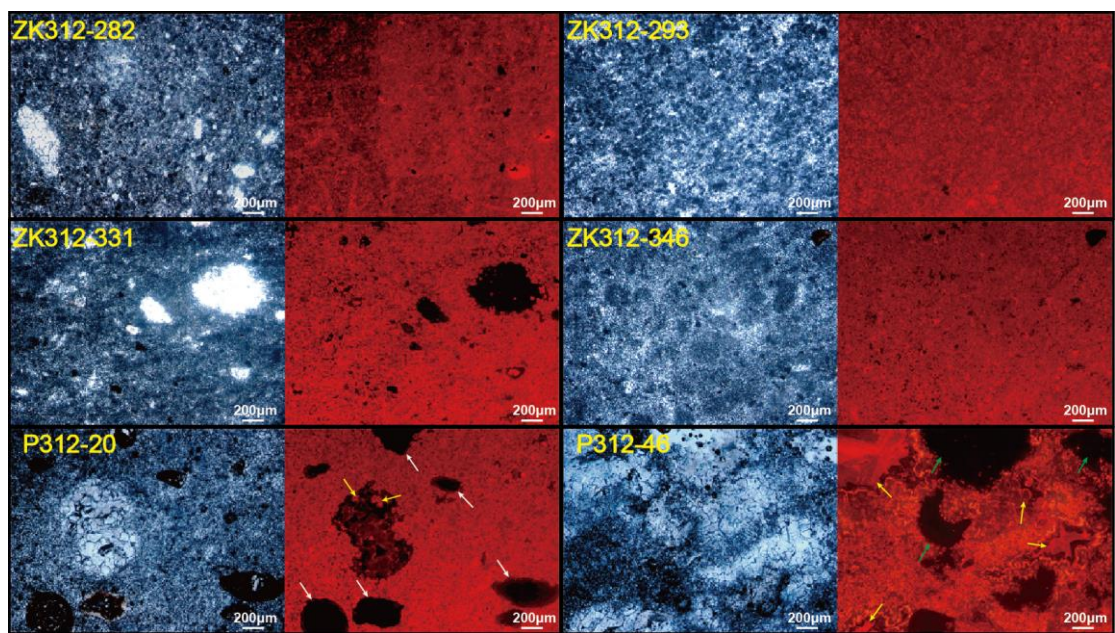


Fig. S6. Polarized light (PL; left) and cathodoluminescent (CL; right) images of four typical samples from >50 m depth (ZK312-282, ZK312-293, ZKE312-331 and ZK312-346) and 2 typical samples from <50 m depth (P312-20 and P312-46). The CL images of samples from >50 m depth show no obvious cements. The samples from <50 m depth contain large phosphatic patches (pointed by white arrows), chalcedony block (pointed by green arrows) and dolomite cements (pointed by yellow arrows).

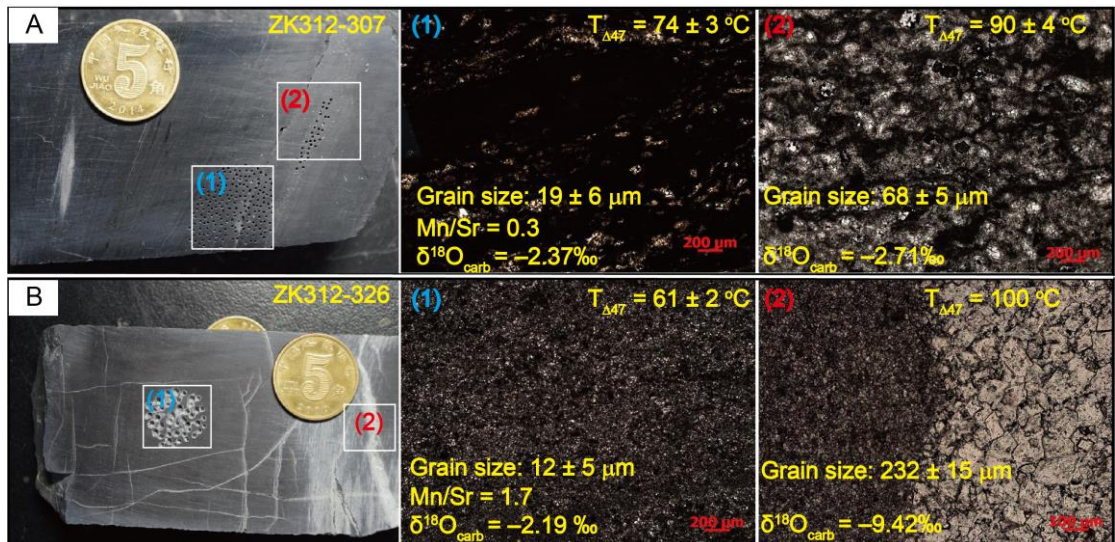


Fig. S7. Typical carbonate textures as observed in the sample slab and under microscopy. (A) Sample ZK312-307 includes major microcrystalline dolomite area [labeled as (1)] and minor coarse crystallite dolomite area [labeled as (2)]. (B) Sample ZK312-326 includes major microcrystalline dolomite area [labeled as (1)] and minor veins [labeled as (2)]. In this study, we sampled the microcrystalline dolomite area by micro-drilling while avoiding those coarse crystallite dolomites and veins for sampling. Geochemical proxies for late diagenesis (i.e., Mn/Sr, $\delta^{18}\text{O}_{\text{dol}}$, and grain size) and corresponding $T_{\Delta 47}$ data are shown for references, as available. Scale: 5-jiao coin is 2.0 cm in diameter.

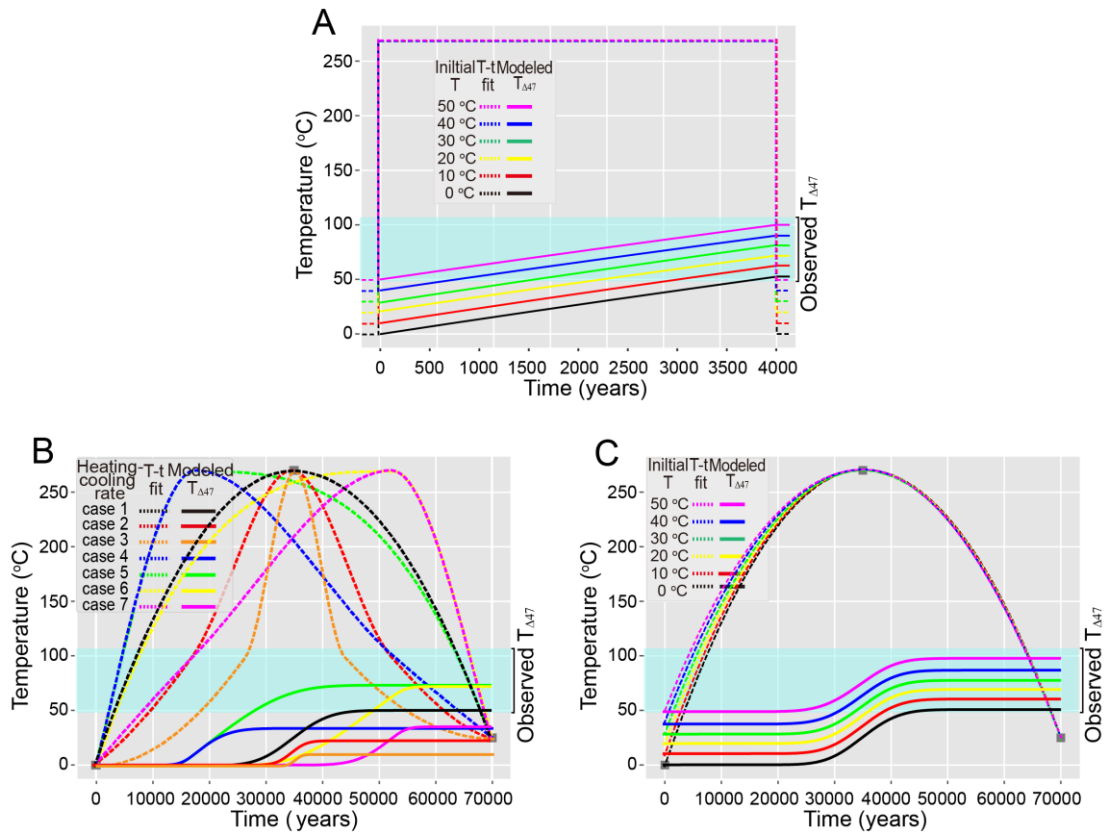


Fig. S8. Solid-state reordering modeling of the study Doushantuo Formation based on the dolomite-based “transient defect/equilibrium defect” model (7-8) and the “equilibrium defect” (9) models, which can achieve the $T_{\Delta 47}$ values (50-106 °C) observed in this study. (A) Dolomite-based “transient defect/equilibrium defect” model (an instantaneous isothermal heating model) results assuming a varying initial temperature from 0 to 50 °C, a heating duration of 4000 years at a peak temperature of 270 °C. (B) “Equilibrium defect” model results for short-duration (70000 years) of hydrothermal events. These simulations assumed an initial temperature of 0 °C, a heating duration of 70000 years at a peak temperature of 270 °C with variable heating-cooling rates, including three symmetric heating-cooling cases (case 1-3) and four asymmetric heating-cooling cases (case 4-7). (C) “Equilibrium defect” model results assuming a varying initial temperature from 0 to 50 °C, a heating duration of 70000 years at a peak temperature of 270 °C, and a fixed heating-cooling rate (i.e., case 1 in B). In subfigures B and C, the “T-t fit” lines denote assumed heating T-time paths, while the “Modeled $T_{\Delta 47}$ ” lines denote the corresponding $T_{\Delta 47}$ evolution of the Doushantuo dolomites predicted by a solid-state reordering model. The shallow blue bands represent the range of measured $T_{\Delta 47}$ values of well-preserved Doushantuo dolomites in this study. See main text for more modeling details.

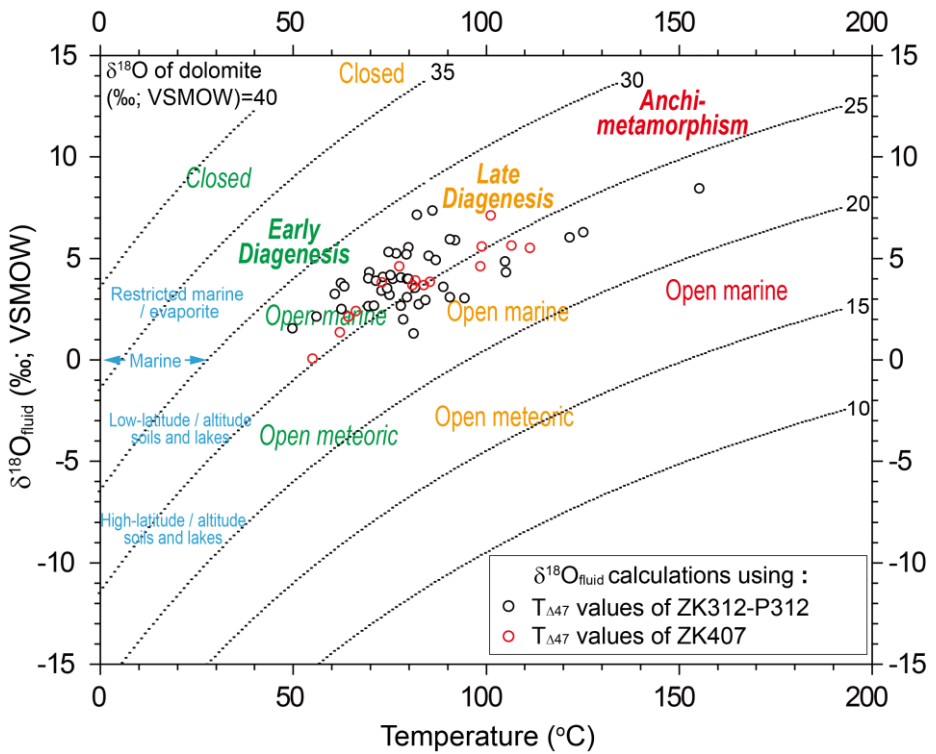


Fig. S9. Originally calculated $\delta^{18}\text{O}$ compositions of the diagenetic fluids ($\delta^{18}\text{O}_{\text{fluid}}$) versus paired $T_{\Delta 47}$ data for Doushantuo dolomite. Recrystallization environments (colored text: early or late diagenetic or anchi-metamorphic) except for those modern environments (blue texts) are either closed (i.e., rock-buffered) or open (i.e., fluid-buffered). Reference isotopic compositions for carbonates and co-existing diagenetic fluids equilibrated over a range of geological conditions were adopted from ref. 10, but updated to the $\delta^{18}\text{O}$ compositions of dolomite. See Methods for further explanation of calculations and the text for detailed interpretations.

ZK312-279

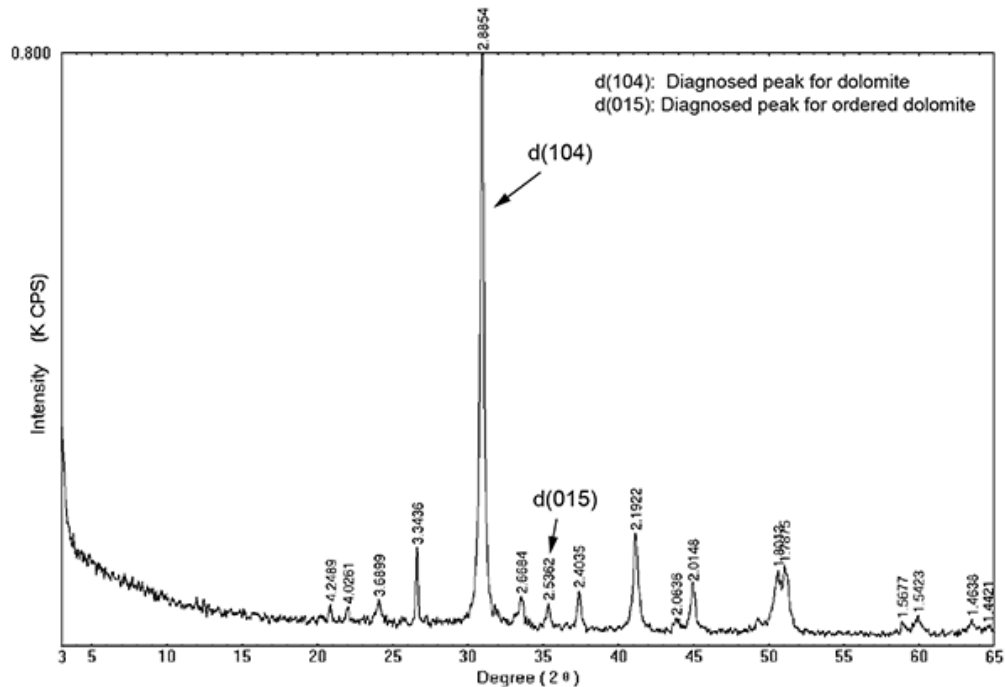


Fig. S10. Representative X-ray diffraction (XRD) spectrum for the Doushantuo Formation (sample ZK312-279). XRD spectra indicate that all study samples consist dominantly of ordered dolomite.

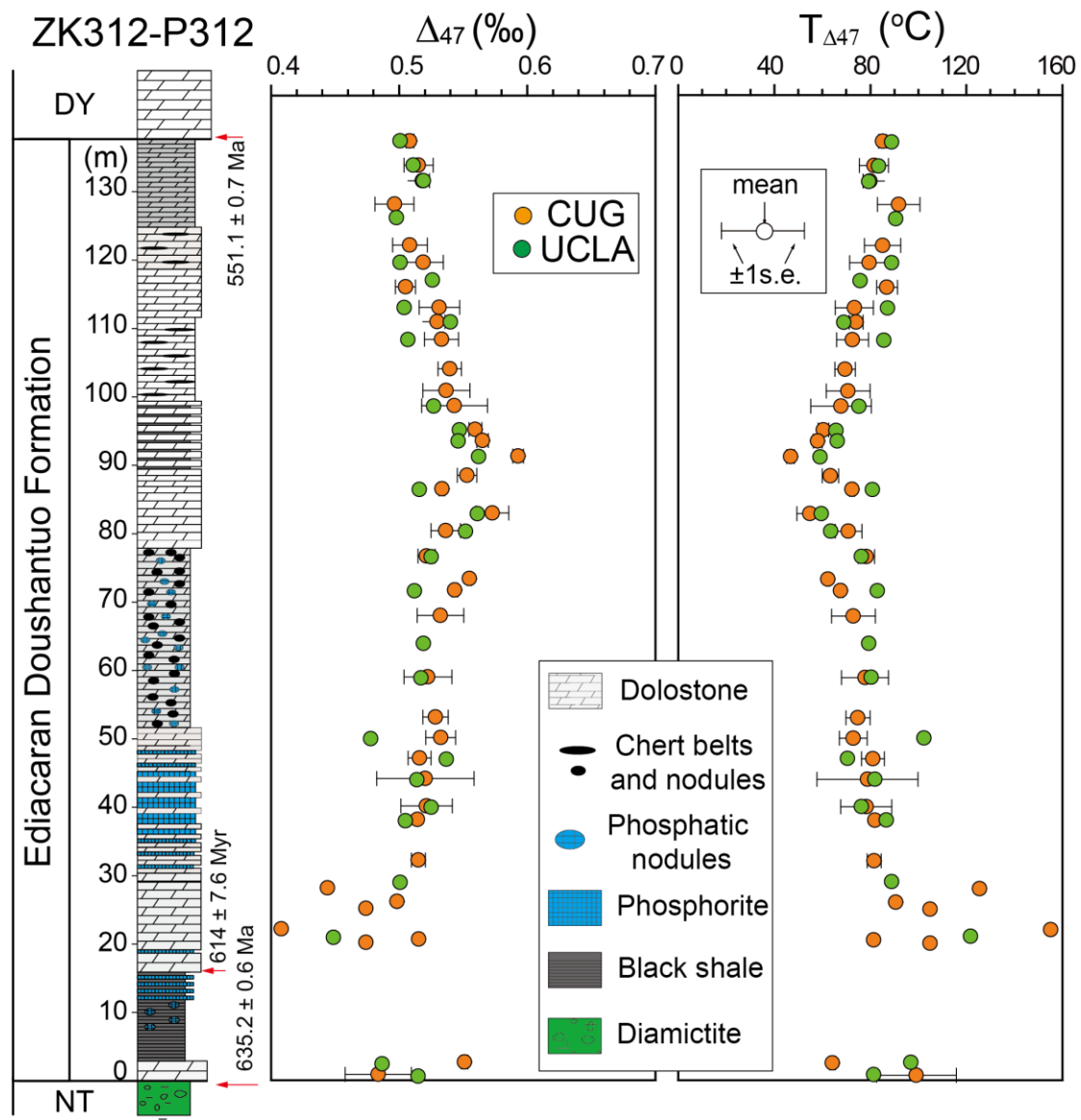


Fig. S11. Comparison of Δ_{47} and $T_{\Delta_{47}}$ data measured at University of California-Los Angeles (UCLA) (green symbols) and at China University of Geosciences-Wuhan (CUG-W) (orange symbols). The two datasets show almost the same values and stratigraphic trends through the Doushantuo Formation, confirming the robustness of our Δ_{47} and $T_{\Delta_{47}}$ data. NT = Nantuo Formation, DY = Dengying Formation.

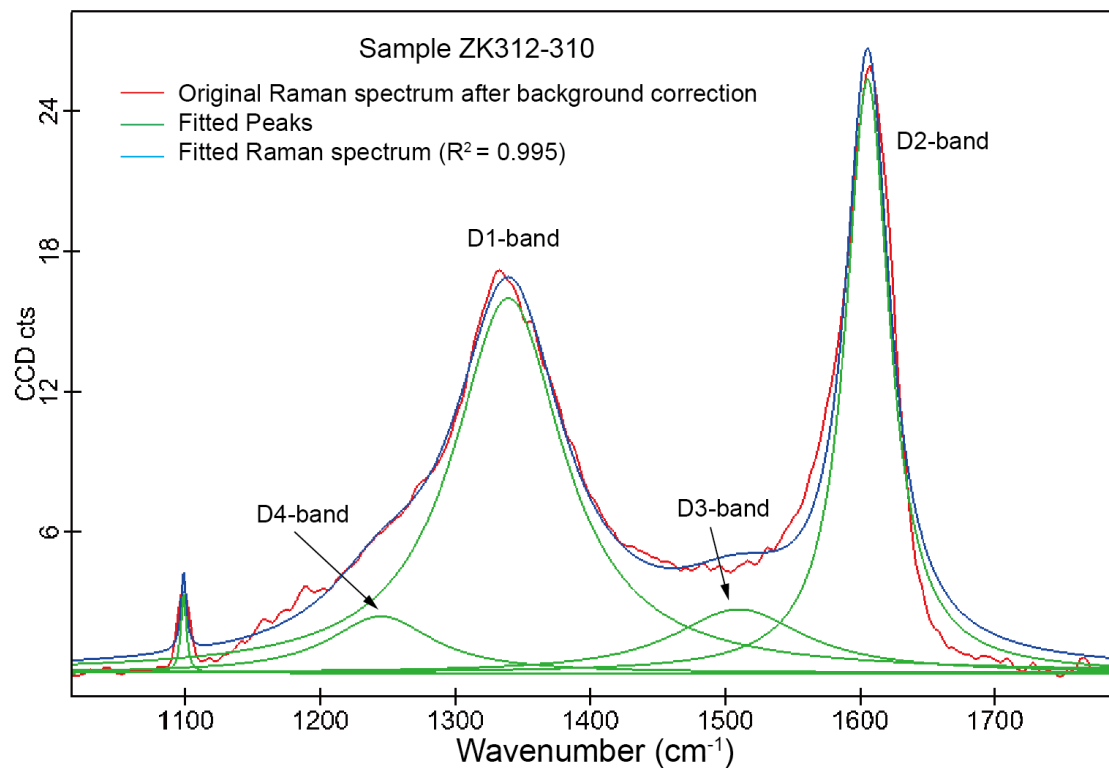


Fig. S12. Representative Raman spectra of organic matter (OM) of Doushantuo sample ZK312-310. Four discriminative bands (D1, D2, D3, and D4; green) are marked. The method of peak decomposition was adopted from ref. 11. The coefficient of variation ($R^2 = 0.995$) compares the original spectrum (red) with the fitted Raman spectrum (blue). CCD cts = charge-coupled device counts.

Table S1. Composite temperature- or diagenesis-related geochemical and petrographic data of dolomites from the Doushantuo Formation.

Sample ID	Height in ZK312-P312 (m)	Δ_{47} (‰) ^a	$T_{\Delta 47}$ (°C) ^b	$T_{\Delta 47}$ (°C) ^c	$T_{\Delta 47}$ (°C) ^d	$T_{\Delta 47}$ (°C) ^e	$T_{\Delta 47}$ (°C) ^f	Initial $T_{\Delta 47}$ (°C) by modeling ^g	Initial $T_{\Delta 47}$ (°C) by modeling ^h	avg. $\delta^{13}\text{C}_{\text{carb}}$ (VPDB, ‰)	avg. $\delta^{18}\text{O}_{\text{carb}}$ (VPDB, ‰)	$\delta^{18}\text{O}_{\text{fluid}}$ (VSMOW, ‰) ⁱ	$\delta^{18}\text{O}_{\text{fluid}}$ (VSMOW, ‰) ^j	Grain size (µm)	Grain size 1 s.d. (µm)	Dolomite (wt %) ^k	Raman of OM FWHM-D1 (cm ⁻¹)	Raman of OM FWHM-D2 (cm ⁻¹)	Peak heating Temperature based on D1 (°C)	Peak heating temperature based on D2 (°C)	Average peak heating temperatures of D1 and D2 (°C)	$R_{\text{o, mv}}$ (%)	R_{o} (%)	Peak heating temperature based on R_{o} (°C)	
ZK312-275	137.3	0.507	107	90	100	114	86	34	36	2.2	-2.0	7.4	-0.1			95									
ZK312-279	133.8	0.515	102	86	95	108	82	29	32	0.2	-1.7	7.2	-0.7	10	4	95	97.4	64.5	260	269	264				
ZK407-270	132.4	0.485	121	103	114	132	99	47	50	6.0	-5.1	5.6	-0.9	49	16										
ZK312-282	131.5	0.519	99	84	93	106	80	27	29	-0.4	-3.0	5.6	-2.5	17	8	91	86.5	66.2	265	292	279				
ZK312-286	128.1	0.497	113	96	106	122	92	40	43	0.5	-4.0	5.9	-1.1	10	4	91	93.4	65.1	253	277	265				
ZK312-288	126.1	0.499	112	95	105	121	91	38	41	0.3	-3.9	6.0	-1.1	8	3	93							3.5	2.58	275
ZK312-293	122.1	0.509	105	89	99	113	85	33	35	2.2	-4.0	5.2	-2.4	11	4	98	87.9	65.9	288	289	289				
ZK312-296	119.6	0.514	102	87	96	109	82	30	32	1.9	-6.0	2.8	-5.1	14	6	93	91.7	65.4	281	281	281				
ZK407-290	119.3	0.473	130	110	122	143	106	55	58	4.9	-5.8	5.6	-0.3	22	9										
ZK312-299	117.0	0.527	94	80	88	100	76	23	25	2.1	-4.0	4.0	-4.5	15	4	98	92.9	65.2	257	278	268				
ZK312-300	116.0	0.506	107	91	100	115	87	34	37	3.3	-4.4	5.0	-2.5	15	4	60									
ZK407-296	115.8	0.486	121	102	113	131	98	46	50	2.8	-6.0	4.6	-1.9												
ZK312-304	113.0	0.525	96	81	89	101	77	24	26	3.8	-2.9	5.3	-3.1	14	5	92	97.6	64.5	262	268	265	4.3	3.05	297	
ZK312-307	110.9	0.532	91	78	86	97	73	20	22	5.4	-3.6	4.1	-4.6	19	6	99							3.0	2.26	258
ZK312-310	108.3	0.529	93	79	87	99	75	22	24	4.8	-2.6	5.4	-3.2	22	8	99	98.3	64.4	265	267	266				

ZK407-310	106.8	0.557	78	66	73	81	62	8	10	1.4	-4.8	1.3	-8.8	16	5	99	96.6	64.7	257	270	264	
ZK312-313	104.0	0.540	87	74	81	92	69	16	18	3.9	-4.5	2.7	-6.5	99	96.6	64.7	257	270	264			
ZK407-317	102.3	0.516	101	86	95	108	81	29	31	-0.3	-4.8	3.9	-4.1	16	5	99	96.6	64.7	257	270	264	
ZK312-317	100.8	0.537	89	75	83	93	71	18	20	4.1	-4.7	2.7	-6.3	8	3	93	101	64.0	283	261	272	
ZK407-320	100.1	0.547	83	71	78	87	66	13	15	-0.1	-4.4	2.4	-7.2	20	6	99	96.6	64.7	257	270	264	
ZK312-321	98.6	0.540	87	74	81	92	69	16	18	4.8	-2.9	4.3	-4.9	5	5	93	87.3	66.0	276	290	283	
ZK407-327	95.9	0.533	91	77	85	96	73	20	22	0.7	-3.9	3.8	-5.0	17	4	99	96.6	64.7	257	270	264	
ZK312-326	95.1	0.556	79	67	73	82	62	9	10	4.6	-2.4	3.8	-6.3	12	5	90	82.4	66.8	272	301	286	
ZK312-328	93.5	0.559	77	65	72	80	61	7	9	4.5	-2.7	3.3	-6.9	13	6	99	96.6	64.7	257	270	264	
ZK312-331	91.2	0.586	64	54	60	65	50	-4	-3	3.0	-2.7	1.6	-10.3	15	6	65	73.8	68.0	274	319	297	
ZK407-337	89.4	0.524	96	81	90	102	77	25	27	-0.4	-3.7	4.6	-3.8	99	96.6	64.7	257	270	264			
ZK312-335	88.4	0.554	80	67	74	83	63	10	11	3.1	-2.7	3.7	-6.3	99	96.6	64.7	257	270	264			
ZK312-339	86.4	0.528	94	80	88	99	75	22	25	4.0	-3.8	4.2	-4.3	13	4	91	80.4	67.1	261	305	283	
ZK312-346	82.9	0.570	72	61	67	74	56	3	4	2.5	-3.1	2.2	-8.7	18	7	90	74.9	67.9	271	317	294	
ZK407-351	81.2	0.481	124	105	117	136	101	50	53	-4.5	-3.9	7.1	0.8	15	4	99	96.6	64.7	257	270	264	
ZK312-351	80.3	0.540	87	74	81	92	69	16	18	1.0	-3.2	4.1	-5.1	14	4	90	79.8	67.1	270	306	288	
ZK312-356	76.6	0.523	97	82	91	103	78	25	27	4.0	-4.2	4.1	-4.2	99	96.6	64.7	257	270	264			
ZK407-360	73.8	0.509	105	89	99	113	85	33	35	0.8	-5.4	3.8	-3.8	22	9	99	96.6	64.7	257	270	264	
ZK312-361	73.3	0.556	79	67	73	82	62	9	10	3.8	-3.7	2.5	-7.6	99	96.6	64.7	257	270	264			
ZK312-364	71.6	0.536	89	76	83	94	71	18	20	2.9	-3.5	4.0	-5.0	22	8	35	99	96.6	64.7	257	270	264
ZK312-368	67.9	0.533	91	77	85	96	73	20	22	2.9	-4.2	3.5	-5.4	22	8	75	91.6	65.4	262	281	272	
ZK312-376	63.9	0.520	98	83	92	105	79	27	29	3.4	-3.3	5.3	-2.9	99	96.6	64.7	257	270	264			
ZK312-384	58.9	0.522	97	82	91	103	78	26	28	3.6	-6.3	2.0	-6.2	99	96.6	64.7	257	270	264			
ZK407-398	57.8	0.517	100	85	94	107	81	28	31	1.4	-5.0	3.7	-4.3	16	4	99	96.6	64.7	257	270	264	
P312-8	53.0	0.529	93	79	87	99	75	22	24	0.7	-4.7	3.2	-5.4	14	4	93	96.6	64.7	257	270	264	

ZK407-412p	50.4	0.512	103	88	97	111	83	31	33	0.6	-5.3	3.6	-4.1	15	5				
P312-14	50.0	0.520	98	83	92	105	79	27	29	0.3	-4.5	4.0	-4.1			97			
P312-20	47.0	0.519	99	84	93	106	80	27	29	-0.6	-4.5	4.0	-4.1			97			
ZK407-416	46.1	0.573	70	59	65	72	55	1	2	-1.2	-5.0	0.1	-11.0						
P312-26	44.0	0.520	98	83	92	105	79	27	29	-3.6	-5.3	3.1	-5.0			80			
P312-32	40.0	0.523	97	82	91	103	78	25	27	-0.8	-5.5	2.7	-5.6			93			
P312-37	38.0	0.511	104	88	97	111	84	32	34	0.1	-6.0	3.0	-4.7	60	23	93			
ZK407-424	35.4	0.552	81	68	75	84	64	11	12	-7.5	-4.4	2.1	-7.8	18	6				
P312-46	32.1	0.516	101	86	95	108	81	29	31	4.2	-5.1	3.6	-4.4	20	7	98			
ZK407-428	31.1	0.465	137	115	128	151	111	60	64	-1.3	-6.4	5.5	-0.1	33	11				
P312-53	29.0	0.502	110	93	103	118	89	37	39	4.8	-5.9	3.6	-3.6	86	26	98			
P312-55	28.0	0.445	154	129	144	172	125	75	79	4.0	-6.8	6.4	1.6						
P312-58	26.0	0.499	112	95	105	121	91	38	41	4.4	-6.6	3.1	-4.0						
P312-60	25.0	0.475	129	109	121	141	105	53	57	4.7	-6.4	4.9	-1.1			98			
P312-66	22.0	0.409	191	158	179	221	155	106	112	4.7	-7.0	8.5	5.1			98			
P312-67	21.0	0.450	149	125	140	167	122	71	75	4.8	-6.8	6.1	1.1			98			
P312-68	20.5	0.516	101	86	95	108	81	29	31	5.0	-7.3	1.4	-6.6						
P312-70	20.0	0.475	129	109	121	141	105	53	57	4.6	-6.9	4.3	-1.7			98			
P312-105	2.5	0.530	93	79	87	98	74	21	23	1.6	-4.3	3.6	-5.1	98	97.1	64.6	287	269	278
P312-114	0.7	0.492	116	99	109	126	95	43	46	-0.1	-7.1	3.1	-3.7	98	107	63.1	254	248	251

^a We used Δ_{47} to replace the STF- $\Delta_{47\text{ARF}25}$. The STF- $\Delta_{47\text{ARF}25}$ value was calibrated by applying the Standards Transfer Function to average $\Delta_{47\text{ARF}25}$ value. The average $\Delta_{47\text{ARF}25}$ value was calculated using the repeated $\Delta_{47\text{ARF}25}$ values. The $\Delta_{47\text{ARF}25}$ value was calculated from Brand raw Δ_{47} value by applying it to the absolute reference frame (12) and then scaling it to a 25 °C phosphoric acid reaction by addition of a 0.082‰ temperature correction factor for 90 °C reactions (13). The Brand raw Δ_{47} value was calculated by converting our measured raw δ_{45} , raw δ_{46} , raw δ_{47} , raw δ_{48} and raw δ_{49} values into the Brand parameter frame (14, 15) (details see Table S3).

^b The $T_{\Delta_{47}}$ values were calculated using the calcite temperature calibration in ref. 16.

^cThe $T_{\Delta 47}$ values were calculated using the calcite temperature calibration in ref. 17.

^dThe $T_{\Delta 47}$ values were calculated using the dolomite temperature calibration in ref. 18.

^eThe $T_{\Delta 47}$ value was calculated using the Brand parameter-based calcite temperature calibration in ref. 19.

^fThe $T_{\Delta 47}$ values were calculated using the revised dolomite temperature calibration in this study.

^gThe initial $T_{\Delta 47}$ value was derived from the modeling of the solid-state reordering effects by assuming a peak heating temperature of 270 °C for **2000** years based on the $T_{\Delta 47}$ values in this study and the exchange-diffusion kinetic model from ref. 8 (see text for details).

^hThe initial $T_{\Delta 47}$ value was derived from the modeling of the solid-state reordering effects by assuming a peak heating temperature of 270 °C for **4000** years based on the $T_{\Delta 47}$ values in this study and the transient defect/equilibrium defect model in ref. 7 (see text for details).

ⁱThe $\delta^{18}\text{O}_{\text{fluid}}$ (VSMOW, ‰) value was calculated using the $T_{\Delta 47}$ value which was calculated by using the revised dolomite temperature calibration in this study.

^jThe $\delta^{18}\text{O}_{\text{fluid}}$ (VSMOW, ‰) value was calculated using the initial $T_{\Delta 47}$ value from modeling which is based on an exchange-diffusion kinetic solid-state reordering model in ref. 8 by assuming a hydrothermal event with a peak heating of 270°C for 2000 years (see text for details).

^kData were generated by XRD with an uncertainty of ca. ±5%.

Table S2. The summarized Δ_{47} values (CUG and UCLA) and $T_{\Delta47}$ values of dolomite samples from the Doushantuo Formation in this study.

Analysis #	Date	Laboratory	Sample ID	Height (m)	$\delta^{13}\text{C}$ (VPDB, ‰)	$\delta^{18}\text{O}$ (VPDB, ‰)	$\Delta_{47\text{ARF25}}$ (%)	STDEV. $\Delta_{47\text{ARF25}}$ (%) ^a	Average Δ_{47} (%)	n	Average Δ_{47} 1 s.d. (%) ^b	Average Δ_{47} 1 s.e. (%) ^c	$T_{\Delta47}$ (°C)	$T_{\Delta47}$ 1 s.e. (°C)	
ZK312-P312 section															
49355	150925-34	CUG	ZK312-275	137.3	2.11	-2.87	0.531	0.515	0.507	4	0.0054	0.003	86	2	
49025	150908-22	CUG	ZK312-275		2.17	-2.61	0.523	0.507							
	201512	UCLA	ZK312-275		2.34	-0.01		0.502							
49035	150908-23	CUG	ZK312-275		2.28	-2.37	0.521	0.505							
49365	150925-35	CUG	ZK312-279	133.8	0.10	-1.78	0.537	0.521	0.515	4	0.0161	0.008	82	4	
49055	150908-25	CUG	ZK312-279		0.06	-1.77	0.548	0.532							
	201512	UCLA	ZK312-279		0.31	-1.63		0.512							
49870	151011-34	CUG	ZK312-279		0.19	-1.65	0.510	0.494							
5255	20190215-2	CUG	ZK312-282	131.5	-0.24	-2.90	0.513	0.517	0.519	5	0.0099	0.004	80	2	
5420	20190218-4	CUG	ZK312-282		-0.22	-2.94	0.506	0.504							
5610	20190222-4	CUG	ZK312-282		-0.22	-3.09	0.524	0.524							
	201512	UCLA	ZK312-282		-0.43	-2.85		0.520							
56808	160422-21	CUG	ZK312-282		-0.90	-3.16	0.534	0.530							
49105	150912-21	CUG	ZK312-286	128.1	0.47	-3.99	0.498	0.482	0.497	2	0.0210	0.015	92	8	
49375	150925-36	CUG	ZK312-286		0.52	-4.10	0.528	0.512							
	201512	UCLA	ZK312-288	126.1	0.27	-3.86		0.499	0.499	1				91	
49115	150912-22	CUG	ZK312-293	122.1	2.30	-4.01	0.499	0.483	0.509	3	0.0236	0.014	85	7	

49155	150912-26	CUG	ZK312-313	104.0	3.95	-4.90	0.566	0.549	0.540	2	0.0130	0.009	69	4
49476	150929-31	CUG	ZK312-313		3.88	-4.08	0.547	0.531						
49486	150929-32	CUG	ZK312-317	100.8	4.15	-4.93	0.536	0.520	0.537	3	0.0317	0.018	71	8
57206	160503-33	CUG	ZK312-317		4.20	-4.60	0.573	0.574						
59167	160528-E4	CUG	ZK312-317		3.92	-4.46	0.522	0.518						
49165	150914-31	CUG	ZK312-321	98.6	4.84	-3.24	0.534	0.518	0.540	4	0.0375	0.019	70	9
49496	150929-33	CUG	ZK312-321		4.85	-2.98	0.534	0.518						
	201512	UCLA	ZK312-321		4.89	-2.90		0.528						
60193	160614-G3	CUG	ZK312-321		4.56	-2.56	0.593	0.595						
57273	160503-35	CUG	ZK312-326	95.1	4.46	-2.71	0.556	0.555	0.556	3	0.0083	0.005	62	2
	201512	UCLA	ZK312-326		4.91	-2.35		0.548						
58459	160520-C1	CUG	ZK312-326		4.45	-2.24	0.565	0.565						
49513	150929-34	CUG	ZK312-328	93.5	4.46	-3.03	0.587	0.570	0.559	3	0.0118	0.007	61	3
	201512	UCLA	ZK312-328		4.76	-2.54		0.547						
59177	160528-E5	CUG	ZK312-328		4.20	-2.59	0.562	0.561						
49523	150929-35	CUG	ZK312-331	91.2	3.14	-3.01	0.601	0.585	0.586	4	0.0163	0.008	50	3
58908	160522-D1	CUG	ZK312-331		2.81	-2.45	0.595	0.597						
	201512	UCLA	ZK312-331		3.29	-2.70		0.563						
58928	160522-D2	CUG	ZK312-331		2.80	-2.76	0.596	0.598						
49185	150914-33	CUG	ZK312-335	88.4	3.02	-3.03	0.577	0.561	0.554	2	0.0102	0.007	63	3
49537	150930-36	CUG	ZK312-335		3.16	-2.41	0.563	0.546						
49195	150914-34	CUG	ZK312-339	86.4	4.08	-4.50	0.552	0.536	0.528	3	0.0104	0.006	75	3
	201512	UCLA	ZK312-339		4.04	-3.29		0.517						
49547	151001-31	CUG	ZK312-339		3.90	-3.46	0.548	0.532						
59317	160602-F3	CUG	ZK312-346	82.9	2.12	-2.94	0.584	0.585	0.570	4	0.0189	0.009	56	4

	201512	UCLA	P312-32		-0.71	-5.44		0.526						
49703	151005-34	CUG	P312-37	38.0	0.04	-6.11	0.531	0.515	0.511	2	0.0065	0.005	84	2
	201512	UCLA	P312-37		0.19	-5.95		0.506						
49258	150916-25	CUG	P312-46	32.1	4.08	-5.67	0.528	0.512	0.516	5	0.0123	0.005	82	3
49713	151005-35	CUG	P312-46		4.48	-4.55	0.532	0.516						
58968	160522-D5	CUG	P312-46		4.16	-4.30	0.505	0.499						
59040	160522-D6	CUG	P312-46		4.09	-5.61	0.536	0.533						
60233	160614-G4	CUG	P312-46		4.05	-5.54	0.523	0.518						
	201512	UCLA	P312-53	29.0	4.76	-5.94		0.502	0.502	1			89	
49730	151005-36	CUG	P312-55	28.0	4.00	-6.84	0.461	0.445	0.445	1			125	
49820	151009-35	CUG	P312-58	26.0	4.45	-6.64	0.515	0.498	0.499	2	0.0008	0.001	91	0
49975	151012-36	CUG	P312-58		4.33	-6.57	0.516	0.500						
49740	151007-31	CUG	P312-60	25.0	4.68	-6.39	0.491	0.475	0.475	1			105	
49750	151007-32	CUG	P312-66	22.0	4.72	-7.00	0.425	0.409	0.409	1			155	
	201512	UCLA	P312-67	21.0	4.78	-6.79		0.450	0.450	1			122	
49268	150916-26	CUG	P312-68	20.5	4.97	-7.28	0.533	0.516	0.516	1			81	
49765	151007-33	CUG	P312-70	20.0	4.63	-6.94	0.491	0.475	0.475	1			105	
49785	151009-32	CUG	P312-105	2.5	1.93	-4.04	0.565	0.549	0.530	3	0.0369	0.021	74	10
7894	170325-5	UCLA	P312-105		1.27	-4.65	0.504	0.488						
49830	151009-36	CUG	P312-105		1.47	-4.08	0.570	0.554						
49288	150916-31	CUG	P312-114	0.7	0.02	-7.06	0.523	0.507	0.492	4	0.0395	0.020	94	11
49800	151009-33	CUG	P312-114		-0.13	-6.94	0.529	0.513						
7707	170321-4	CUG	P312-114		-0.63	-7.55	0.452	0.433						
	201512	UCLA	P312-114		0.18	-6.73		0.516						

ZK407 section

9244	170418-3	CUG	ZK407-270	132.4	6.14	-4.80	0.497	0.480	0.485	3	0.0243	0.014	99	8
9504	170422-6	CUG	ZK407-270		6.03	-5.12	0.481	0.463						
9524	170423-2	CUG	ZK407-270		5.89	-5.42	0.526	0.511						
9294	170419-6	CUG	ZK407-290	119.3	4.88	-5.70	0.466	0.448	0.473	4	0.0520	0.026	106	16
9494	170422-5	CUG	ZK407-290		4.80	-6.06	0.452	0.433						
11232	170601-4	CUG	ZK407-290		4.88	-5.64	0.561	0.549						
11302	170603-2	CUG	ZK407-290		5.02	-5.96	0.479	0.461						
10872	170525-2	CUG	ZK407-296	115.8	1.72	-6.19	0.510	0.495	0.486	3	0.0233	0.013	98	8
10962	170526-5	CUG	ZK407-296		3.26	-6.08	0.477	0.459						
11122	170529-3	CUG	ZK407-296		3.32	-5.79	0.518	0.503						
10882	170525-3	CUG	ZK407-310	106.8	0.93	-4.80	0.607	0.597	0.557	4	0.0294	0.015	62	6
10972	170527-1	CUG	ZK407-310		1.57	-4.64	0.559	0.546						
11132	170529-4	CUG	ZK407-310		1.54	-4.71	0.542	0.528						
11212	170601-2	CUG	ZK407-310		1.45	-4.98	0.569	0.556						
9224	170418-1	CUG	ZK407-317	102.3	-0.49	-5.15	0.562	0.549	0.516	4	0.0446	0.022	82	11
9484	170422-4	CUG	ZK407-317		-0.33	-4.97	0.504	0.488						
9594	170424-6	CUG	ZK407-317		-0.09	-4.23	0.485	0.468						
11192	170530-5	CUG	ZK407-317		-0.26	-5.02	0.570	0.558						
10902	170525-5	CUG	ZK407-320	100.1	-0.07	-4.38	0.511	0.496	0.547	4	0.0373	0.019	66	8
10982	170527-2	CUG	ZK407-320		-0.02	-4.42	0.559	0.547						
11152	170530-1	CUG	ZK407-320		-0.09	-4.42	0.593	0.582						
11242	170601-5	CUG	ZK407-320		-0.07	-4.22	0.577	0.565						
9234	170418-2	CUG	ZK407-327	95.9	0.75	-3.58	0.516	0.500	0.533	4	0.0254	0.013	73	6
9474	170422-3	CUG	ZK407-327		0.65	-4.00	0.545	0.531						
9544	170424-1	CUG	ZK407-327		0.74	-4.03	0.553	0.540						

11222	170601-3	CUG	ZK407-327		0.78	-3.85	0.574	0.562												
7055	20180303-2	CUG	ZK407-337	89.4	-0.49	-3.75	0.479	0.487	0.524	4	0.0251	0.013	77	6						
8465	20180401-5	CUG	ZK407-337		-0.32	-3.50	0.526	0.533												
9698	20180428-3	CUG	ZK407-337		-0.39	-3.71	0.537	0.544												
9848	20180501-4	CUG	ZK407-337		-0.41	-3.74	0.524	0.532												
9254	170419-2	CUG	ZK407-351	81.2	-4.46	-3.62	0.497	0.481	0.481	2	0.0143	0.010	101	6						
9454	170422-1	CUG	ZK407-351		-4.63	-4.13	0.498	0.482												
9284	170419-5	CUG	ZK407-360	73.8	0.88	-5.06	0.521	0.506	0.509	2	0.0244	0.017	85	9						
9444	170421-6	CUG	ZK407-360		0.69	-5.64	0.526	0.511												
9274	170419-4	CUG	ZK407-398	57.8	1.51	-4.70	0.563	0.551	0.517	3	0.0290	0.017	81	8						
9434	170421-5	CUG	ZK407-398		1.39	-5.06	0.514	0.498												
9554	170424-2	CUG	ZK407-398		1.43	-5.15	0.518	0.503												
9304	170419-7	CUG	ZK407-412P	50.4	0.70	-4.87	0.500	0.484	0.512	3	0.0247	0.014	84	7						
9424	170421-4	CUG	ZK407-412P		0.58	-5.42	0.544	0.530												
9564	170424-3	CUG	ZK407-412p		0.51	-5.68	0.535	0.521												
10912	170525-6	CUG	ZK407-416	46.1	-1.20	-5.22	0.604	0.593	0.573	4	0.0213	0.011	55	4						
11082	170528-4	CUG	ZK407-416		-1.22	-4.98	0.581	0.569												
11162	170530-2	CUG	ZK407-416		-1.22	-5.16	0.558	0.545												
11272	170602-3	CUG	ZK407-416		-1.16	-4.75	0.596	0.585												
10922	170526-1	CUG	ZK407-424	35.4	-7.48	-4.33	0.533	0.518	0.552	4	0.0289	0.014	64	6						
11102	170529-1	CUG	ZK407-424		-7.44	-4.52	0.556	0.543												
11172	170530-3	CUG	ZK407-424		-7.57	-4.26	0.598	0.587												
11252	170602-1	CUG	ZK407-424		-7.61	-4.31	0.571	0.558												
10932	170526-2	CUG	ZK407-428	31.1	-1.23	-6.28	0.449	0.430	0.465	3	0.0307	0.018	111	11						
11112	170529-2	CUG	ZK407-428		-1.31	-6.49	0.498	0.482												

11182	170530-4	CUG	ZK407-428	-1.22	-6.46	0.500	0.484
-------	----------	-----	-----------	-------	-------	-------	-------

^a In order to simplify the description, we use Δ_{47} to replace the STF- $\Delta_{47\text{ARF25}}$ (more details see Table S3).

^b Standard deviations (s.d.) correspond to duplicate analyses.

^c Standard error (s.e.) was given by s.d./($n^{0.5}$).

Table S3. Raw data, Δ_{47} values and other related values of absolute reference frame (ARF) and the standards in this study.

Analysis-#	Date	Sample ID	raw δ_{45} (‰, WG ^a)	raw δ_{46} (‰, WG ^a)	raw δ_{47} (‰, WG ^a)	raw δ_{48} (‰, WG ^a)	raw δ_{49} (‰, WG ^a)	Brand raw Δ_{47} (‰) ^b	Brand raw Δ_{48} (‰) ^b	Brand raw Δ_{49} (‰) ^b	Slope _{EGL} ^c	Slope _{ETF} ^d	Intercept _{ETF} ^d	$\Delta_{47, \text{ARF25}}$ (‰) ^e	Average $\Delta_{47, \text{ARF25}}$ (‰) ^f	Expected $\Delta_{47, \text{ARF25}}$ (‰) ^f	Δ_{47} (STF - $\Delta_{47, \text{ARF25}}$) ^g
48910	150830-32	Equilibrated CO ₂ at 10 °C	-0.447	-12.074	-12.318	-27.740	6.083	0.009	-3.829	30.877	0.003	1.139	0.915				
48900	150830-31	Equilibrated CO ₂ at 10 °C	-0.351	-12.165	-12.288	-27.801	4.995	0.030	-3.709	29.842	0.003	1.139	0.915				
48920	150830-33	Equilibrated CO ₂ at 10 °C	0.186	4.244	4.434	9.801	4.853	0.068	1.283	-3.672	0.003	1.139	0.915				
48732	150824-31	Equilibrated CO ₂ at 10 °C	17.851	-12.349	6.152	-27.864	2.724	0.100	-3.401	8.325	0.003	1.139	0.915				
48442	150815-31	Equilibrated CO ₂ at 10 °C	17.795	-11.804	6.617	-26.568	4.692	0.075	-3.173	9.267	0.003	1.139	0.915				
48452	150815-32	Equilibrated CO ₂ at 10 °C	18.137	-3.267	15.504	-7.252	4.265	0.060	-0.733	-8.431	0.003	1.139	0.915				
48742	150824-32	Equilibrated CO ₂ at 10 °C	18.175	-3.211	15.674	-7.097	3.226	0.133	-0.690	-9.606	0.003	1.139	0.915				
48467	150815-33	Equilibrated CO ₂ at 10 °C	18.126	-1.182	17.658	-2.043	2.611	0.135	0.321	-14.109	0.003	1.139	0.915				
48755	150824-33	Equilibrated CO ₂ at 10 °C	18.271	-0.717	18.222	-1.426	2.862	0.085	0.008	-14.914	0.003	1.139	0.915				

48477	150815-34	Equilibrated CO ₂ at 10 °C	18.440	4.198	23.358	9.808	3.588	0.121	1.383	-23.834	0.003	1.139	0.915
48765	150824-34	Equilibrated CO ₂ at 10 °C	18.540	4.606	23.905	10.864	3.420	0.153	1.615	-24.880	0.003	1.139	0.915
48193	150802-11	Equilibrated CO ₂ at 25 °C	-0.552	-14.900	-15.255	-33.317	5.683	-0.045	-3.852	36.400	0.003	1.139	0.915
48203	150802-12	Equilibrated CO ₂ at 25 °C	-0.491	-14.561	-14.862	-32.432	6.104	-0.047	-3.626	36.066	0.003	1.139	0.915
48213	150802-13	Equilibrated CO ₂ at 25 °C	-0.481	-14.741	-15.022	-32.762	6.581	-0.040	-3.602	36.918	0.003	1.139	0.915
48222	150802-14	Equilibrated CO ₂ at 25 °C	-0.181	-5.588	-5.697	-12.198	1.065	-0.018	-1.064	12.343	0.003	1.139	0.915
48232	150802-15	Equilibrated CO ₂ at 25 °C	-0.116	-5.520	-5.597	-12.267	3.868	-0.051	-1.271	14.972	0.003	1.139	0.915
48242	150802-16	Equilibrated CO ₂ at 25 °C	-0.224	-5.604	-5.763	-12.384	6.145	-0.024	-1.221	17.559	0.003	1.139	0.915
48252	150806-21	Equilibrated CO ₂ at 25 °C	-0.053	-2.819	-2.837	-6.300	-0.581	-0.011	-0.673	5.035	0.003	1.139	0.915
48262	150806-24	Equilibrated CO ₂ at 25 °C	0.180	1.934	2.085	4.436	4.239	-0.002	0.562	0.242	0.003	1.139	0.915
48327	150811-31	Equilibrated CO ₂ at 25 °C	17.650	-15.108	3.107	-33.851	2.854	0.024	-3.982	14.229	0.003	1.139	0.915
48337	150811-32	Equilibrated CO ₂ at 25 °C	18.048	-5.671	12.997	-12.891	4.065	0.053	-1.600	-3.819	0.003	1.139	0.915
48347	150811-33	Equilibrated CO ₂	18.197	-2.890	15.891	-6.303	2.957	0.008	-0.533	-10.519	0.003	1.139	0.915

at 25 °C													
		Equilibrated CO ₂ at 25 °C	18.340	1.736	20.752	4.087	3.582	0.085	0.609	-19.018	0.003	1.139	0.915
48357	150811-34	Equilibrated CO ₂ at 25 °C	17.685	-14.792	3.456	-33.435	4.116	0.021	-4.192	14.829	0.003	1.139	0.915
48586	150819-31	Equilibrated CO ₂ at 25 °C	18.020	-5.717	12.920	-13.111	5.119	0.051	-1.728	-2.653	0.003	1.139	0.915
48596	150819-32	Equilibrated CO ₂ at 25 °C	18.114	-3.031	15.711	-6.855	4.814	0.055	-0.806	-8.325	0.003	1.139	0.915
48606	150819-34	Equilibrated CO ₂ at 25 °C	18.358	1.822	20.849	4.390	4.168	0.078	0.740	-18.629	0.003	1.139	0.915
48712	150824-14	Equilibrated CO ₂ at 50 °C	29.853	-13.593	17.028	-30.887	5.283	0.006	-3.994	0.843	0.003	1.139	0.915
48407	150814-12	Equilibrated CO ₂ at 50 °C	17.696	-16.651	1.536	-37.691	3.641	-0.048	-4.824	18.110	0.003	1.139	0.915
48417	150814-13	Equilibrated CO ₂ at 50 °C	17.675	-15.663	2.501	-35.207	5.169	-0.051	-4.258	17.671	0.003	1.139	0.915
48427	150814-14	Equilibrated CO ₂ at 50 °C	17.818	-12.756	5.566	-28.832	5.451	-0.044	-3.573	11.921	0.003	1.139	0.915
48541	150819-11	Equilibrated CO ₂ at 50 °C	17.247	-28.181	-10.479	-63.150	3.414	-0.062	-8.028	42.245	0.003	1.139	0.915
48551	150819-12	Equilibrated CO ₂ at 50 °C	17.648	-16.551	1.584	-37.410	6.814	-0.051	-4.738	21.174	0.003	1.139	0.915
48561	150819-13	Equilibrated CO ₂ at 50 °C	17.740	-13.150	5.091	-29.692	7.289	-0.045	-3.661	14.649	0.003	1.139	0.915

48571	150819-14	Equilibrated CO ₂ at 50 °C	17.826	-13.069	5.251	-29.638	7.153	-0.054	-3.769	14.256	0.003	1.139	0.915
48692	150824-11	Equilibrated CO ₂ at 50 °C	17.249	-28.888	-11.213	-64.974	4.703	-0.090	-8.517	45.077	0.003	1.139	0.915
48702	150824-13	Equilibrated CO ₂ at 50 °C	29.937	-12.632	18.061	-28.561	3.945	-0.020	-3.545	-2.487	0.003	1.139	0.915
48722	150824-13	Equilibrated CO ₂ at 50 °C	17.244	-28.148	-10.461	-63.591	6.748	-0.073	-8.562	45.643	0.003	1.139	0.915
48833	150830-11	Equilibrated CO ₂ at 50 °C	-1.100	-28.028	-28.824	-63.470	5.704	-0.163	-8.679	64.732	0.003	1.139	0.915
48843	150830-12	Equilibrated CO ₂ at 50 °C	-1.071	-26.644	-27.422	-60.504	6.770	-0.150	-8.366	62.850	0.003	1.139	0.915
48853	150830-13	Equilibrated CO ₂ at 50 °C	-0.392	-8.765	-9.085	-20.096	5.924	-0.067	-2.689	23.904	0.003	1.139	0.915
48866	150830-14	Equilibrated CO ₂ at 50 °C	-0.386	-10.541	-10.874	-24.079	5.476	-0.118	-3.174	27.054	0.003	1.139	0.915
48083	150801-11	Heated CO ₂ at 1000 °C	18.124	-4.719	13.181	-10.182	0.543	-0.784	-0.774	-9.258	0.003	1.139	0.915
48093	150801-12	Heated CO ₂ at 1000 °C	18.139	-4.557	13.418	-10.312	2.626	-0.725	-1.229	-7.528	0.003	1.139	0.915
48118	150801-14	Heated CO ₂ at 1000 °C	18.093	-4.540	13.364	-10.053	1.013	-0.748	-1.003	-9.110	0.003	1.139	0.915
48103	150801-13	Heated CO ₂ at 1000 °C	22.000	-19.490	2.332	-42.678	2.450	-0.760	-4.241	18.116	0.003	1.139	0.915
48128	150801-15	Heated CO ₂ at	22.113	-18.964	2.969	-41.742	3.746	-0.767	-4.336	18.236	0.003	1.139	0.915

		1000 °C											
		Heated CO ₂ at 1000 °C	21.994	-19.352	2.475	-42.679	1.453	-0.751	-4.524	16.826	0.003	1.139	0.915
48146	150801-16	Heated CO ₂ at 1000 °C	-0.103	-1.669	-2.575	-3.727	4.862	-0.829	-0.392	8.277	0.003	1.139	0.915
48156	150801-17	Heated CO ₂ at 1000 °C	-0.086	-1.724	-2.563	-4.151	5.046	-0.781	-0.707	8.552	0.003	1.139	0.915
48166	150801-18	Heated CO ₂ at 1000 °C	-0.681	-15.911	-17.156	-35.826	5.492	-0.834	-4.396	38.438	0.003	1.139	0.915
48276	150802-11-R	Heated CO ₂ at 1000 °C	-0.310	-8.140	-9.143	-18.423	4.999	-0.831	-2.246	21.606	0.003	1.139	0.915
48286	150802-15-R	Heated CO ₂ at 1000 °C	-0.211	-7.034	-7.924	-16.208	5.356	-0.798	-2.221	19.626	0.003	1.139	0.915
48301	150802-23-R	Heated CO ₂ at 1000 °C	-0.010	-5.898	-6.628	-13.528	5.466	-0.824	-1.789	17.231	0.003	1.139	0.915
48311	150802-26-R	Heated CO ₂ at 1000 °C	17.963	-5.644	12.107	-13.075	4.802	-0.766	-1.839	-3.052	0.003	1.139	0.915
48392	150811-33-R	Heated CO ₂ at 1000 °C	17.652	-14.474	2.941	-33.061	5.999	-0.776	-4.450	16.122	0.003	1.139	0.915
48511	150814-14-R	Heated CO ₂ at 1000 °C	17.630	-14.258	3.141	-32.340	4.686	-0.770	-4.143	14.382	0.003	1.139	0.915
48521	150815-31-R	Heated CO ₂ at 1000 °C	17.893	-5.435	12.255	-12.499	4.233	-0.756	-1.675	-3.955	0.003	1.139	0.915
48639	150819-11-R	Heated CO ₂ at 1000 °C	17.192	-27.313	-10.420	-62.045	5.985	-0.825	-8.630	43.142	0.003	1.139	0.915

48649	150819-14-R	Heated CO ₂ at 1000 °C	17.557	-14.955	2.389	-33.823	4.975	-0.751	-4.262	16.163	0.003	1.139	0.915
48778	150824-11-R	Heated CO ₂ at 1000 °C	17.127	-28.593	-11.775	-64.549	5.359	-0.833	-8.669	45.268	0.003	1.139	0.915
48788	150824-14-R	Heated CO ₂ at 1000 °C	29.620	-15.014	14.614	-34.632	4.678	-0.719	-4.977	3.321	0.003	1.139	0.915
48798	150824-13-R	Heated CO ₂ at 1000 °C	29.318	-13.848	15.469	-31.373	3.956	-0.738	-3.978	0.583	0.003	1.139	0.915
48811	150824-31-R	Heated CO ₂ at 1000 °C	17.513	-14.544	2.744	-33.414	5.116	-0.763	-4.672	15.518	0.003	1.139	0.915
48821	150824-34-R	Heated CO ₂ at 1000 °C	18.220	-0.920	17.132	-2.285	4.274	-0.735	-0.447	-13.081	0.003	1.139	0.915
48975	150830-11-R	Heated CO ₂ at 1000 °C	-1.266	-27.908	-29.547	-63.490	6.840	-0.857	-8.946	65.864	0.003	1.139	0.915
48985	150830-12-R	Heated CO ₂ at 1000 °C	-1.012	-25.936	-27.376	-59.009	7.121	-0.877	-8.231	61.636	0.003	1.139	0.915
49065	150910-31	NBS-19	30.438	2.807	33.831	6.633	2.743	-0.412	1.005	-34.114	0.003	1.139	0.915
49085	150910-32	NBS-19	30.512	3.010	34.131	7.155	2.835	-0.394	1.120	-34.483	0.003	1.139	0.915
49318	150925-31	NBS-19	30.565	3.058	34.224	7.661	-2.765	-0.405	1.525	-40.018	0.003	1.139	0.915
49328	150925-32	NBS-19	30.669	3.370	34.612	8.372	0.658	-0.440	1.609	-37.415	0.003	1.139	0.915
49850	151011-31	NBS-19	30.640	3.292	34.480	7.557	4.452	-0.461	0.957	-33.588	0.003	1.139	0.915
49985	151014-31	NBS-19	30.635	3.394	34.588	7.622	4.111	-0.453	0.817	-34.106	0.003	1.139	0.915
50003	151014-32	NBS-19	30.491	2.953	34.064	6.700	3.172	-0.382	0.782	-34.030	0.003	1.139	0.915
50013	151014-33	NBS-19	30.515	2.978	34.076	6.748	3.829	-0.419	0.777	-33.469	0.003	1.139	0.915
50023	151014-34	NBS-19	30.703	3.514	34.814	10.120	2.045	-0.419	3.058	-36.387	0.003	1.139	0.915
													0.395
													0.378

49075	150910-33	NBS-19	30.562	3.338	34.477	7.738	3.263	-0.432	1.044	-34.743	0.003	1.139	0.915	0.381	0.364
49095	150910-34	NBS-19	30.551	3.265	34.410	7.555	3.667	-0.414	1.007	-34.205	0.003	1.139	0.915	0.402	0.386
Analysis#	Date	Sample ID	raw δ_{45} (‰,WG ^a)	raw δ_{46} (‰,WG ^a)	raw δ_{47} (‰,WG ^a)	raw δ_{48} (‰,WG ^a)	raw δ_{49} (‰,WG ^a)	Brand raw Δ_{47} (‰) ^b	Brand raw Δ_{48} (‰) ^b	Brand raw Δ_{49} (‰) ^b	Slope _{GL} ^c	Slope _{TF} ^d	Intercept _{TF} ^d	$\Delta_{47\text{ARF25}}$ (‰) ^e	Mean $\Delta_{47\text{ARF25}}$ (‰)
															Expected $\Delta_{47\text{ARF25}}$ (‰) ^f
															Δ_{47}
															(STF- $\Delta_{47\text{ARF25}}$) (‰) ^g
56662	160415-32	Equilibrated CO ₂ at 50 °C	-0.755	-22.415	-22.913	-50.110	6.387	-0.113	-6.050	53.079	0.001	1.124	0.908		
56682	160415-34	Equilibrated CO ₂ at 50 °C	17.839	-5.662	12.651	-12.965	8.223	-0.086	-1.691	0.508	0.001	1.124	0.908		
56891	160415-31	Equilibrated CO ₂ at 50 °C	-1.153	-26.983	-27.821	-61.244	12.546	-0.132	-8.456	69.775	0.001	1.124	0.908		
56948	160415-32	Equilibrated CO ₂ at 50 °C	28.457	-22.071	6.928	-50.693	8.109	-0.084	-7.359	22.312	0.001	1.124	0.908		
56968	160421-34	Equilibrated CO ₂ at 50 °C	29.184	-7.257	22.707	-16.490	-5.606	-0.053	-2.058	-21.705	0.001	1.124	0.908		
56978	160415-32	Heated CO ₂ at 1000 °C	-0.775	-22.555	-23.751	-52.095	9.928	-0.809	-7.843	57.104	0.001	1.124	0.908		
56988	160415-24	Heated CO ₂ at 1000 °C	30.119	-0.040	30.275	-0.671	5.729	-0.741	-0.590	-25.487	0.001	1.124	0.908		
56998	160422-26	Heated CO ₂ at 1000 °C	18.040	-4.947	12.848	-12.002	9.043	-0.801	-2.153	-0.302	0.001	1.124	0.908		
57008	160415-31	Heated CO ₂ at 1000 °C	-1.009	-26.204	-27.581	-60.311	11.231	-0.821	-9.058	66.543	0.001	1.124	0.908		

57088	160421-32	Heated CO ₂ at 1000 °C	28.408	-22.154	6.101	-51.661	8.692	-0.774	-8.204	23.125	0.001	1.124	0.908				
57098	160421-34	Heated CO ₂ at 1000 °C	29.040	-8.815	20.286	-20.948	7.114	-0.735	-3.456	-5.980	0.001	1.124	0.908				
57166	160503-31	ISTB-1	18.140	-3.109	15.326	-7.561	6.323	-0.275	-1.361	-6.712	0.001	1.124	0.908	0.659	0.713	0.726	0.667
57392	160506-16	ISTB-1	18.164	-3.088	15.412	-7.534	5.816	-0.234	-1.375	-7.277	0.001	1.124	0.908	0.704			0.716
57607	160509-46	ISTB-1	18.144	-3.044	15.438	-7.558	5.871	-0.232	-1.487	-7.288	0.001	1.124	0.908	0.706			0.719
58028	160514-02	ISTB-1	17.976	-3.663	14.642	-8.966	2.920	-0.236	-1.666	-8.819	0.001	1.124	0.908	0.703			0.715
58038	160515-A1	ISTB-1	17.977	-3.733	14.571	-9.313	4.468	-0.238	-1.875	-7.153	0.001	1.124	0.908	0.701			0.713
58133	160516-B1	ISTB-1	18.244	-3.173	15.418	-7.796	3.970	-0.225	-1.469	-9.016	0.001	1.124	0.908	0.714			0.727
58527	160520-B1	ISTB-1	18.081	-3.410	15.012	-8.220	3.219	-0.228	-1.422	-9.127	0.001	1.124	0.908	0.712			0.724
58918	160522-B1	ISTB-1	18.117	-3.520	14.923	-8.545	4.141	-0.243	-1.528	-8.039	0.001	1.124	0.908	0.695			0.706
59022	160522-B3	ISTB-1	18.135	-3.282	15.193	-7.712	0.957	-0.230	-1.167	-11.667	0.001	1.124	0.908	0.709			0.721
59197	160522-B4	ISTB-1	17.975	-3.914	14.390	-9.601	4.074	-0.235	-1.801	-7.184	0.001	1.124	0.908	0.705			0.717
59553	160605-B8	ISTB-1	18.054	-3.599	14.830	-8.900	4.699	-0.192	-1.727	-7.265	0.001	1.124	0.908	0.753			0.769
59603	160606-B1	ISTB-1	18.199	-3.248	15.306	-8.006	2.588	-0.217	-1.530	-10.188	0.001	1.124	0.908	0.724			0.737
59749	160608-E8	ISTB-1	18.010	-3.732	14.586	-9.147	4.318	-0.256	-1.709	-7.337	0.001	1.124	0.908	0.681			0.690
59944	160610-E10	ISTB-1	16.092	-8.306	8.171	-18.621	-3.059	-0.130	-2.113	-3.677	0.001	1.124	0.908	0.831			0.855
59964	160611-F6	ISTB-1	18.277	-3.423	15.197	-8.300	4.650	-0.230	-1.476	-7.890	0.001	1.124	0.908	0.709			0.721
60158	160614-B3	ISTB-1	18.133	-3.359	15.070	-8.220	4.176	-0.273	-1.523	-8.334	0.001	1.124	0.908	0.661			0.669
56724	160415-23	ISTB-1	18.104	-2.987	15.491	-7.150	8.296	-0.196	-1.192	-4.966	0.001	1.124	0.908	0.746			0.762
56734	160415-24	ISTB-1	18.136	-3.025	15.462	-7.321	11.423	-0.220	-1.288	-1.839	0.001	1.124	0.908	0.720			0.734
56881	160422-26	NBS-19	30.264	3.060	33.830	6.512	5.677	-0.487	0.381	-31.594	0.001	1.124	0.908	0.394	0.394	0.378	0.378
57243	160503-36	NBS-19	30.040	2.579	33.129	5.668	5.906	-0.469	0.500	-30.237	0.001	1.124	0.908	0.414			0.400
57303	160504-26	NBS-19	30.413	3.293	34.221	7.239	5.060	-0.486	0.639	-32.779	0.001	1.124	0.908	0.394			0.378

57527	160507-46	NBS-19	30.156	2.773	33.411	6.121	5.112	-0.502	0.565	-31.486	0.001	1.124	0.908	0.376	0.359	
57887	160512-46	NBS-19	30.284	3.039	33.823	6.781	4.370	-0.492	0.691	-32.831	0.001	1.124	0.908	0.387	0.371	
58048	160515-A3	NBS-19	30.170	2.597	33.244	5.559	4.756	-0.505	0.357	-31.508	0.001	1.124	0.908	0.374	0.356	
58262	160514-16	NBS-19	30.410	3.212	34.182	7.246	2.706	-0.442	0.806	-34.889	0.001	1.124	0.908	0.443	0.432	
58331	160516-A1	NBS-19	30.130	2.706	33.344	6.277	2.054	-0.476	0.853	-34.280	0.001	1.124	0.908	0.406	0.392	
58419	160520-A2	NBS-19	30.275	2.705	33.470	6.239	3.453	-0.498	0.818	-33.075	0.001	1.124	0.908	0.381	0.365	
58606	160522-A1	NBS-19	30.363	2.956	33.844	6.850	4.275	-0.470	0.924	-32.846	0.001	1.124	0.908	0.413	0.398	
58948	160522-A3	NBS-19	30.264	2.813	33.532	6.500	3.006	-0.534	0.861	-33.699	0.001	1.124	0.908	0.341	0.321	
59110	160522-A4	NBS-19	30.291	2.802	33.590	6.359	3.792	-0.492	0.743	-32.947	0.001	1.124	0.908	0.388	0.371	
59419	160603-A7	NBS-19	30.345	2.936	33.799	6.777	4.208	-0.475	0.892	-32.854	0.001	1.124	0.908	0.406	0.392	
59613	160606-A1	NBS-19	30.437	3.121	34.101	7.242	0.891	-0.457	0.984	-36.490	0.001	1.124	0.908	0.426	0.413	
59663	160607-C9	NBS-19	30.304	2.821	33.618	6.435	3.376	-0.498	0.780	-33.397	0.001	1.124	0.908	0.382	0.365	
59829	160609-E7	NBS-19	30.364	2.940	33.836	6.752	3.270	-0.463	0.858	-33.785	0.001	1.124	0.908	0.420	0.406	
59879	160610-E9	NBS-19	30.292	2.824	33.630	6.675	3.434	-0.477	1.013	-33.335	0.001	1.124	0.908	0.405	0.390	
60024	160612-F5	NBS-19	30.278	2.691	33.419	6.303	3.318	-0.536	0.910	-33.180	0.001	1.124	0.908	0.339	0.318	
60044	160612-F7	NBS-19	30.152	2.303	32.915	5.282	5.098	-0.517	0.669	-30.601	0.001	1.124	0.908	0.361	0.342	
60088	160613-A1	NBS-19	30.367	2.949	33.835	6.897	3.716	-0.476	0.984	-33.375	0.001	1.124	0.908	0.405	0.391	
56744	160415-25	NBS-19	30.336	3.282	34.158	6.849	8.757	-0.459	0.273	-29.122	0.001	1.124	0.908	0.424	0.411	
56754	160415-26	NBS-19	30.217	3.075	33.788	6.510	9.707	-0.495	0.348	-27.695	0.001	1.124	0.908	0.384	0.368	

^aWG: working gas. These are raw values relative to a reference gas with $\delta^{13}\text{C} = -29.85\text{\textperthousand}$ (VPDB) and $\delta^{18}\text{O} = -5.31\text{\textperthousand}$ (VPDB).

^b The Brand raw Δ_{47} , raw Δ_{48} and raw Δ_{49} values were calculated by converting our measured raw δ_{45} , raw δ_{46} , raw δ_{47} , raw δ_{48} and raw δ_{49} values within the Brand parameter frame ([14-15](#)).

^c Slope_{EGL}: the slope of Equilibrated Gas Line (EGL) of our laboratory following the method of [ref. 12](#).

^d Slope_{ETF} and Intercept_{ETF}: the slope and intercept of Empirical Transfer Function (ETF) of our laboratory following the method of [ref. 12](#).

^e $\Delta_{47\text{ARF}25}$ was calculated from Brand raw Δ_{47} value by applying it to the Absolute Reference Frame (ARF, which includes the values of Slope_{EGL}, Slope_{ETF} and Intercept_{ETF}) of our laboratory following the method of ref. 12 and then scaling to a 25 °C phosphoric acid reaction by addition of a 0.082‰ temperature correction factor for 90 °C reactions (ref. 13).

^f The expected $\Delta_{47\text{ARF}25}$ value was the long-term observed value or the reported value based on the four ETH standards (ETH-1: 0.258 ‰, ETH-2: 0.256 ‰, EHT-3: 0.693 ‰ and ETH-4: 0.507 ‰) in ref. 17. In this study, two standards were used, one is international standard (NBS-19) and another is in-house standard (ISTB-1), and their expected values are 0.378 ‰ and 0.726 ‰, respectively.

^g The STF- $\Delta_{47\text{ARF}25}$ value was calibrated by applying the Standards Transfer Function (STF) to its average $\Delta_{47\text{ARF}25}$ value. The STF was built by comparing the observed average $\Delta_{47\text{ARF}25}$ values to their expected $\Delta_{47\text{ARF}25}$ values. In order to simplify the description, here we use Δ_{47} to replace the STF- $\Delta_{47\text{ARF}25}$ and also in the paper.

Table S4. The total organic carbon (TOC), major and trace elements data of whole rocks from the Doushantuo Formation, and rare earth elements + Yttrium (REE+Y) concentration data of the whole rock and the carbonate fraction.

Height in ZK312-P312 (m)	Sample ID	Major		Trace		REE+Y of the whole rock (ppm)															
		TOC (%) ^a	element (ppm)	element (ppm)																	
				Mn	Sr	Th	La	Ce	Pr	Nd	Sm	Eu	Gd	Tb	Dy	Y	Ho	Er	Tm	Yb	Lu
137.3	ZK312-275	0.36	39	49	0.16	1.31	2.00	0.32	1.37	0.26	0.07	0.30	0.05	0.27	2.29	0.05	0.17	0.02	0.13	0.02	
133.8	ZK312-279	0.28	34	75	0.19	2.45	3.30	0.50	2.36	0.51	0.10	0.52	0.07	0.42	4.00	0.09	0.30	0.03	0.22	0.03	
131.5	ZK312-282		87	121	0.36	3.04	4.98	0.81	3.42	0.70	0.17	0.72	0.10	0.60	5.04	0.12	0.33	0.05	0.26	0.04	
128.1	ZK312-286	0.37	46	82	0.18	2.25	2.71	0.50	2.20	0.39	0.09	0.34	0.05	0.32	2.84	0.06	0.19	0.03	0.17	0.02	
126.1	ZK312-288	0.55	57	85	0.56	2.85	4.28	0.64	2.71	0.56	0.13	0.52	0.07	0.45	3.60	0.10	0.30	0.04	0.27	0.03	
122.1	ZK312-293	0.04	56	47	0.17	1.80	3.16	0.48	2.04	0.40	0.10	0.43	0.06	0.36	2.95	0.07	0.19	0.03	0.15	0.02	
119.6	ZK312-296		70	90	0.30	2.32	4.46	0.63	2.59	0.60	0.12	0.54	0.09	0.52	3.84	0.11	0.31	0.05	0.31	0.05	
116.9	ZK312-299	0.13	62	92	0.46	3.96	6.84	1.00	4.22	0.85	0.19	0.95	0.13	0.77	6.22	0.14	0.40	0.07	0.36	0.04	
116.0	ZK312-300	0.11	40	56	0.51	3.27	5.67	0.86	3.91	0.83	0.20	0.79	0.13	0.79	6.48	0.15	0.45	0.07	0.37	0.05	
113.0	ZK312-304	1.02	51	101	1.32	8.71	14.10	2.02	8.86	1.87	0.40	1.93	0.28	1.76	14.75	0.34	0.99	0.14	0.90	0.12	
110.9	ZK312-307	0.69	24	93	0.53	5.58	7.60	1.09	4.66	0.87	0.19	0.96	0.15	0.91	9.51	0.19	0.59	0.08	0.45	0.05	
108.3	ZK312-310		24	93	0.11	2.64	4.27	0.67	3.01	0.67	0.15	0.73	0.12	0.71	7.31	0.16	0.39	0.06	0.24	0.04	
104.0	ZK312-313	0.11	48	54	0.33	2.11	2.98	0.50	2.20	0.44	0.08	0.43	0.06	0.37	2.99	0.08	0.23	0.03	0.20	0.03	
100.8	ZK312-317	0.02	68	38	0.12	1.71	2.65	0.42	1.75	0.35	0.09	0.36	0.05	0.30	2.03	0.06	0.16	0.02	0.13	0.02	
98.6	ZK312-321	0.03	96	52	0.16	2.61	3.71	0.70	3.11	0.59	0.13	0.60	0.08	0.45	3.15	0.08	0.21	0.03	0.15	0.02	
95.1	ZK312-326		81	48	0.14	1.88	2.48	0.47	2.00	0.42	0.10	0.40	0.07	0.36	2.51	0.07	0.17	0.03	0.15	0.02	
93.0	ZK312-328		89	51	0.19	1.84	3.15	0.53	2.17	0.45	0.12	0.47	0.08	0.46	3.17	0.08	0.24	0.03	0.17	0.02	
91.2	ZK312-331	0.13	79	59	0.13	1.04	1.72	0.30	1.41	0.37	0.07	0.39	0.06	0.34	2.72	0.07	0.20	0.02	0.14	0.02	

88.5	ZK312-335	0.25	111	118	0.75	4.28	7.52	1.26	5.77	1.34	0.31	1.33	0.20	1.21	7.87	0.22	0.61	0.09	0.48	0.07
86.5	ZK312-339	0.23	101	48	0.19	1.31	2.38	0.34	1.50	0.33	0.09	0.37	0.05	0.31	2.36	0.06	0.17	0.02	0.15	0.02
83.0	ZK312-346		132	74	0.11	0.93	1.78	0.28	1.08	0.29	0.06	0.30	0.05	0.38	3.21	0.08	0.23	0.03	0.20	0.03
80.3	ZK312-351	0.1	85	125	0.52	3.21	5.27	0.96	4.04	0.96	0.22	0.97	0.15	0.89	6.83	0.19	0.50	0.07	0.38	0.05
76.6	ZK312-356	1.38	122	540	1.39	12.44	21.03	3.34	14.79	3.06	0.77	3.24	0.48	2.87	20.95	0.56	1.52	0.21	1.18	0.16
73.3	ZK312-361	0.9	128	680	0.93	8.95	14.41	2.37	10.23	2.21	0.56	2.41	0.35	2.12	16.52	0.42	1.17	0.15	0.89	0.13
71.6	ZK312-364	1.32	125	595	1.39	10.80	18.47	2.95	13.40	2.93	0.67	3.02	0.47	2.84	21.20	0.53	1.57	0.22	1.20	0.17
67.9	ZK312-368	0.34	87	367	0.09	0.80	1.58	0.27	1.35	0.32	0.07	0.30	0.04	0.27	2.35	0.06	0.17	0.03	0.16	0.02
64.0	ZK312-376	0.3	51	381	0.13	1.05	1.85	0.34	1.52	0.37	0.07	0.35	0.05	0.30	2.48	0.06	0.18	0.03	0.15	0.02
59.0	ZK312-384	1.7	108	256	0.43	6.22	10.45	1.85	8.84	1.99	0.47	2.05	0.30	1.82	16.88	0.38	1.05	0.15	0.74	0.09
53.0	P312-8	0.13	229	50	2.00	4.56	8.68	1.46	6.47	1.55	0.30	1.38	0.25	1.59	10.14	0.34	1.01	0.16	1.00	0.15
50.0	P312-14		311	143	0.03	0.71	0.98	0.18	0.90	0.20	0.05	0.20	0.03	0.22	1.80	0.04	0.13	0.02	0.09	0.01
47.0	P312-20	0.02	419	109	0.14	1.55	2.95	0.42	2.05	0.50	0.11	0.56	0.08	0.52	4.26	0.10	0.27	0.04	0.22	0.03
44.0	P312-26		228	367	0.56	20.70	24.02	5.55	25.92	6.28	1.40	6.98	1.01	6.13	53.81	1.19	3.15	0.40	1.90	0.25
40.0	P312-32	0.12	383	91	0.21	4.95	7.00	1.45	7.29	1.74	0.41	2.15	0.31	1.90	15.85	0.39	1.00	0.14	0.70	0.10
38.5	P312-37		290	126	0.84	15.16	17.82	4.60	22.15	5.08	1.11	5.33	0.74	4.29	31.62	0.82	2.05	0.24	1.30	0.17
32.1	P312-46		840	59	0.07	0.36	4.27	0.07	0.29	0.05	0.02	0.07	0.01	0.05	0.46	0.01	0.04	0.01	0.04	0.01
28.0	P312-53		676	40	0.13	0.45	3.29	0.15	0.61	0.15	0.03	0.14	0.02	0.13	0.76	0.03	0.08	0.01	0.08	0.01
27.0	P312-55		609	31	0.11	0.45	0.86	0.15	0.72	0.17	0.03	0.15	0.02	0.12	0.87	0.02	0.08	0.01	0.05	0.01
25.0	P312-60	0.01	614	36	0.12	0.39	0.72	0.13	0.56	0.12	0.02	0.09	0.01	0.11	0.64	0.02	0.05	0.01	0.05	0.01
22.0	P312-66		320	43	0.10	0.33	0.48	0.08	0.33	0.08	0.02	0.06	0.01	0.07	0.41	0.02	0.05	0.01	0.05	0.01
21.0	P312-68	0.02	265	51	0.55	0.88	1.94	0.32	1.42	0.35	0.05	0.35	0.05	0.32	1.86	0.05	0.21	0.03	0.15	0.03
20.0	P312-70		335	51	0.14	0.50	0.92	0.13	0.49	0.13	0.02	0.09	0.02	0.12	0.58	0.02	0.06	0.01	0.06	0.01
2.5	P312-105	0.02	1844	72	0.59	1.43	3.77	0.34	1.28	0.31	0.07	0.31	0.04	0.27	2.08	0.06	0.18	0.03	0.16	0.03
0.7	P312-114	0.02	808	54	2.17	6.84	11.96	1.32	4.82	1.05	0.23	1.06	0.17	1.13	7.32	0.23	0.70	0.11	0.67	0.10

Height in ZK312-P312 (m)	Sample ID	Major element		Trace element		REE+Y of the carbonate fraction ^b (ppm)													
		(ppm)		(ppm)															
		Mn	Sr	Th	La	Ce	Pr	Nd	Sm	Eu	Gd	Tb	Dy	Y	Ho	Er	Tm	Yb	Lu
137.3	ZK312-275	39	49	0.16	1.30	1.97	0.31	1.35	0.25	0.07	0.29	0.05	0.27	2.26	0.05	0.17	0.02	0.13	0.02
133.8	ZK312-279	34	75	0.19	2.42	3.26	0.50	2.33	0.50	0.10	0.52	0.07	0.41	3.95	0.08	0.29	0.03	0.22	0.03
131.5	ZK312-282	87	121	0.36	2.96	4.86	0.79	3.33	0.68	0.16	0.70	0.10	0.58	4.92	0.12	0.33	0.05	0.26	0.03
128.1	ZK312-286	46	82	0.18	2.22	2.67	0.49	2.17	0.38	0.08	0.34	0.05	0.31	2.81	0.06	0.19	0.03	0.16	0.02
126.1	ZK312-288	57	85	0.56	2.75	4.12	0.62	2.60	0.54	0.12	0.50	0.07	0.44	3.46	0.09	0.29	0.04	0.26	0.03
122.1	ZK312-293	56	47	0.17	1.78	3.12	0.48	2.01	0.40	0.10	0.42	0.06	0.36	2.92	0.07	0.19	0.03	0.15	0.02
119.6	ZK312-296	70	90	0.30	2.27	4.36	0.62	2.53	0.58	0.12	0.53	0.09	0.51	3.76	0.11	0.30	0.05	0.30	0.05
116.9	ZK312-299	62	92	0.46	3.84	6.63	0.97	4.09	0.82	0.19	0.92	0.13	0.74	6.02	0.14	0.39	0.06	0.35	0.04
116.0	ZK312-300	40	56	0.51	3.16	5.47	0.83	3.77	0.80	0.19	0.77	0.13	0.76	6.26	0.14	0.43	0.06	0.35	0.05
113.0	ZK312-304	51	101	1.32	7.92	12.82	1.84	8.06	1.70	0.36	1.76	0.25	1.60	13.41	0.31	0.90	0.13	0.82	0.11
110.9	ZK312-307	24	93	0.53	5.38	7.32	1.05	4.49	0.84	0.19	0.93	0.15	0.87	9.16	0.18	0.57	0.08	0.44	0.05
108.3	ZK312-310	24	93	0.11	2.62	4.24	0.67	2.99	0.66	0.15	0.73	0.12	0.70	7.25	0.16	0.39	0.06	0.24	0.04
104.0	ZK312-313	48	54	0.33	2.06	2.91	0.49	2.15	0.43	0.08	0.42	0.06	0.36	2.93	0.08	0.22	0.03	0.20	0.03
100.8	ZK312-317	68	38	0.12	1.70	2.63	0.42	1.74	0.35	0.09	0.36	0.05	0.30	2.01	0.06	0.16	0.02	0.13	0.02
98.6	ZK312-321	96	52	0.16	2.58	3.67	0.69	3.08	0.58	0.13	0.59	0.08	0.44	3.11	0.08	0.21	0.03	0.15	0.02
95.1	ZK312-326	81	48	0.14	1.86	2.46	0.46	1.98	0.42	0.09	0.40	0.06	0.36	2.48	0.07	0.17	0.03	0.15	0.02
93.0	ZK312-328	89	51	0.19	1.81	3.11	0.53	2.15	0.45	0.12	0.46	0.08	0.45	3.13	0.08	0.24	0.03	0.17	0.02
91.2	ZK312-331	79	59	0.13	1.03	1.71	0.30	1.40	0.36	0.07	0.39	0.06	0.33	2.70	0.07	0.20	0.02	0.14	0.02
88.5	ZK312-335	111	118	0.75	4.06	7.14	1.20	5.47	1.27	0.29	1.26	0.19	1.15	7.46	0.21	0.57	0.09	0.46	0.07
86.5	ZK312-339	101	48	0.19	1.29	2.34	0.33	1.48	0.33	0.09	0.36	0.05	0.31	2.33	0.06	0.17	0.02	0.15	0.02

83.0	ZK312-346	132	74	0.11	0.92	1.77	0.28	1.08	0.29	0.06	0.30	0.05	0.37	3.19	0.08	0.23	0.03	0.19	0.03
80.3	ZK312-351	85	125	0.52	3.10	5.08	0.93	3.90	0.92	0.21	0.94	0.15	0.86	6.59	0.18	0.48	0.06	0.37	0.05
76.6	ZK312-356	122	540	1.39	11.26	19.03	3.02	13.39	2.77	0.70	2.93	0.43	2.60	18.96	0.51	1.38	0.19	1.07	0.14
73.3	ZK312-361	128	680	0.93	8.38	13.49	2.22	9.58	2.07	0.52	2.26	0.32	1.98	15.47	0.39	1.09	0.14	0.83	0.12
71.6	ZK312-364	125	595	1.39	9.77	16.72	2.67	12.13	2.65	0.61	2.74	0.42	2.57	19.19	0.48	1.42	0.20	1.09	0.15
67.9	ZK312-368	87	367	0.09	0.79	1.57	0.27	1.35	0.32	0.07	0.30	0.04	0.27	2.34	0.06	0.17	0.03	0.16	0.02
64.0	ZK312-376	51	381	0.13	1.04	1.84	0.34	1.51	0.36	0.07	0.35	0.05	0.30	2.45	0.06	0.18	0.02	0.15	0.02
59.0	ZK312-384	108	256	0.43	6.04	10.14	1.80	8.57	1.93	0.46	1.99	0.29	1.77	16.38	0.37	1.02	0.14	0.72	0.09
53.0	P312-8	229	50	2.00	3.93	7.49	1.26	5.58	1.34	0.26	1.19	0.21	1.38	8.75	0.29	0.87	0.14	0.86	0.13
50.0	P312-14	311	143	0.03	0.71	0.98	0.18	0.90	0.20	0.05	0.20	0.03	0.22	1.80	0.04	0.13	0.02	0.09	0.01
47.0	P312-20	419	109	0.14	1.53	2.92	0.41	2.03	0.50	0.11	0.55	0.08	0.51	4.22	0.10	0.27	0.04	0.21	0.03
44.0	P312-26	228	367	0.56	19.91	23.10	5.34	24.92	6.03	1.35	6.71	0.97	5.90	51.73	1.14	3.03	0.39	1.83	0.24
40.0	P312-32	383	91	0.21	4.88	6.90	1.43	7.18	1.71	0.40	2.12	0.31	1.87	15.62	0.38	0.99	0.14	0.69	0.10
38.5	P312-37	290	126	0.84	14.29	16.80	4.34	20.88	4.79	1.05	5.02	0.70	4.05	29.81	0.77	1.93	0.23	1.22	0.16
32.1	P312-46	840	59	0.07	0.36	4.25	0.07	0.29	0.05	0.02	0.07	0.01	0.05	0.45	0.01	0.04	0.01	0.04	0.01
28.0	P312-53	676	40	0.13	0.45	3.26	0.15	0.60	0.15	0.03	0.14	0.02	0.12	0.75	0.03	0.08	0.01	0.08	0.01
27.0	P312-55	609	31	0.11	0.45	0.86	0.15	0.72	0.16	0.03	0.15	0.02	0.12	0.87	0.02	0.08	0.01	0.05	0.01
25.0	P312-60	614	36	0.12	0.39	0.71	0.13	0.56	0.12	0.02	0.09	0.01	0.11	0.64	0.02	0.05	0.01	0.05	0.01
22.0	P312-66	320	43	0.10	0.33	0.48	0.08	0.32	0.08	0.02	0.06	0.01	0.07	0.41	0.02	0.05	0.01	0.05	0.01
21.0	P312-68	265	51	0.55	0.84	1.86	0.30	1.36	0.34	0.05	0.34	0.05	0.31	1.79	0.05	0.20	0.03	0.15	0.03
20.0	P312-70	335	51	0.14	0.50	0.91	0.13	0.49	0.13	0.02	0.09	0.02	0.12	0.57	0.02	0.06	0.01	0.06	0.01
2.5	P312-105	1844	72	0.59	1.38	3.62	0.33	1.23	0.29	0.06	0.29	0.04	0.26	2.00	0.06	0.17	0.03	0.16	0.02
0.7	P312-114	808	54	2.17	5.83	10.18	1.12	4.10	0.89	0.20	0.91	0.15	0.97	6.23	0.19	0.60	0.09	0.57	0.08

^aTOC data are from ref. 20. ^bREE concentration in carbonate fraction was calculated through the equation $X_{\text{Sample}} \times (1 - Th_{\text{Sample}} / Th_{\text{PAAS}})$, where X represents the concentration of interested element.

Table S5. Geochemical and petrographic data for samples with different carbonate textures as observed in the sample slab and under microscopy.

Sample ID	Formation	Carbonate texture	Average Δ_{47}^a (‰)	$\delta^{18}\text{O}$ (VPDB, ‰)	Grain size (µm)	1 s.d. of grain size ^b (µm)	$T_{\Delta_{47}}$ (°C)	1 s.e. of $T_{\Delta_{47}}^c$ (°C)
ZK312-29	Dengying	Microcrystalline dolomite	0.512	-4.86	10	4	83	7
ZK312-29	Dengying	Carbonate vein	0.431	-7.72	61	10	137	4
ZK312-282	Doushantuo	Microcrystalline dolomite	0.519	-3.15	17	8	80	3
ZK312-282	Doushantuo	Carbonate vein	0.420	-11.62	182	55	146	
ZK312-293	Doushantuo	Microcrystalline dolomite	0.509	-2.92	11	4	85	7
ZK312-293	Doushantuo	Coarse-crystalline dolomite	0.488	-3.93	59	36	97	14
ZK312-307	Doushantuo	Microcrystalline dolomite	0.531	-2.37	19	6	74	3
ZK312-307	Doushantuo	Coarse-crystalline dolomite	0.501	-2.71	68	5	90	4
ZK312-310	Doushantuo	Microcrystalline dolomite	0.532	-2.29	22	8	73	6
ZK312-310	Doushantuo	Coarse-crystalline dolomite	0.528	-2.84	56	20	75	4
ZK312-317	Doushantuo	Microcrystalline dolomite	0.546	-4.31	8	3	67	12
ZK312-317	Doushantuo	Carbonate vein	0.520	-8.20	247	15	79	11
ZK312-326	Doushantuo	Microcrystalline dolomite	0.560	-2.19	12	5	61	2
ZK312-326	Doushantuo	Carbonate vein	0.484	-9.42	232	15	100	
P312-20	Doushantuo	Microcrystalline dolomite	0.513	-4.33	26	8	83	3
P312-20	Doushantuo	Coarse-crystalline dolomite	0.499	-4.48	26	8	91	4
P312-46	Doushantuo	Microcrystalline dolomite	0.509	-3.75	20	7	85	3
P312-46	Doushantuo	Coarse-crystalline dolomite	0.526	-5.38	111	28	76	4

^aFor simplification, we used Δ_{47} to replace the STF- $\Delta_{47\text{ARF25}}$ here (more details see Table S3).

^bStandard deviation (s.d.) was derived from duplicate analyses.

^cStandard error (s.e.) was given as 1 s.d./($n^{0.5}$).

References

1. Zhang S, et al. (2015) New paleomagnetic results from the Ediacaran Doushantuo Formation in South China and their paleogeographic implications. *Precamb. Res.* 259:130–142.
2. Loyd SJ, et al. (2015) Evolution of Neoproterozoic Wonoka–Shuram Anomaly-aged carbonates: Evidence from clumped isotope paleothermometry. *Precamb. Res.* 264:179–191.
3. Bristow TF, Bonifacie M, Derkowsky A., Eiler JM, Grotzinger JP (2011) A hydrothermal origin for isotopically anomalous cap dolostone cements from south China. *Nature* 474:68–71.
4. Zhang S, et al. (2013) Paleomagnetism of the late Cryogenian Nantuo Formation and paleogeographic implications for the South China Block. *J. Asian Earth Sci.* 72:164–177.
5. Jiang G, Shi X, Zhang S, Wang Y, Xiao S (2011) Stratigraphy and paleogeography of the Ediacaran Doushantuo Formation (ca. 635–551Ma) in South China. *Gondwana Res.* 19(4):831–849.
6. An Z, et al. (2015) Stratigraphic position of the Ediacaran Miaohe biota and its constrains on the age of the upper Doushantuo $\delta^{13}\text{C}$ anomaly in the Yangtze Gorges area, South China. *Precamb. Res.* 271:243–253.
7. Henkes GA, et al. (2014) Temperature limits for preservation of primary calcite clumped isotope paleotemperatures. *Geochimica et Cosmochimica Acta* 139:362–382.
8. Lloyd MK, Ryb U, & Eiler JM (2018) Experimental calibration of clumped isotope reordering in dolomite. *Geochimica et Cosmochimica Acta* 242:1–20.
9. Passey BH & Henkes GA (2012) Carbonate clumped isotope bond reordering and geospeedometry. *Earth and Planetary Science Letters* 351–352:223–236.
10. Eiler JM (2011) Paleoclimate reconstruction using carbonate clumped isotope thermometry. *Quaternary Science Reviews* 30: 3575–3588.
11. Kouketsu Y, et al. (2014) A new approach to develop the Raman carbonaceous material geothermometer for low-grade metamorphism using peak width. *Island Arc* 23:33–50.
12. Dennis KJ, Affek HP, Passey BH, Schrag DP, Eiler JM (2011) Defining an absolute reference frame for ‘clumped’ isotope studies of CO₂. *Geochim. Cosmochim. Acta* 75:7117–7131.
13. Defliese WF, Hren MT, Lohmann KC (2015) Compositional and temperature effects of phosphoric acid fractionation on Δ_{47} analysis and implications for discrepant calibrations. *Chem. Geol.* 396:51–60.
14. Daëron M, Blamart D, Peral M, Affek HP et al. (2016) Absolute isotopic abundance ratios and the accuracy of Δ_{47} measurements. *Chem. Geol.* 441:83–96.
15. Brand WA, Assonov SS, Coplen TB (2010) Correction for the ^{17}O interference in $\delta^{13}\text{C}$ measurements when analyzing CO₂ with stable isotope mass spectrometry (IUPAC Technical Report). *Pure Appl. Chem.* 82:1719–1733.
16. Müller IA, et al. (2019) Calibration of the oxygen and clumped isotope thermometers for (proto-)dolomite based on synthetic and natural carbonates. *Chemical Geology* 525:1–17.

17. Bernasconi SM, et al. (2018) Reducing uncertainties in carbonate clumped isotope analysis through consistent carbonate-based standardization. *Geochem. Geophys. Geosyst.* 19:2895–2914.
18. Bonifacie M, et al. (2017) Calibration of the dolomite clumped isotope thermometer from 25 to 350 °C, and implications for a universal calibration for all (Ca, Mg, Fe)CO₃ carbonates. *Geochim. Cosmochim. Acta* 200:255–279.
19. Petersen SV, et al. (2019) Effects of Improved ¹⁷O Correction on Interlaboratory Agreement in Clumped Isotope Calibrations, Estimates of Mineral - Specific Offsets, and Temperature Dependence of Acid Digestion Fractionation. *Geochemistry, Geophysics, Geosystems* 20:1-25.
20. Li C, et al. (2017) Uncovering the spatial heterogeneity of Ediacaran carbon cycling. *Geobiology* 15:211-224.